Fall 12-8-2021

QUANTUM MECHANICS-BASED COMPUTATIONAL CHEMISTRY HAS BECOME A POWERFUL PARTNER IN THE SCIENTIFIC RESEARCH OF NITROGEN-RICH COMPOUNDS, PAVING THE WAY FOR IMPORTANT ADVANCES IN BIOCHEMICAL, PHARMACOLOGICAL AND OTHER RELATED FIELDS

Dobrushe Denburg
CUNY Bernard M Baruch College

QUANTUM MECHANICS-BASED COMPUTATIONAL CHEMISTRY HAS BECOME A POWERFUL PARTNER IN THE SCIENTIFIC RESEARCH OF NITROGEN-RICH COMPOUNDS, PAVING THE WAY FOR IMPORTANT ADVANCES IN BIOCHEMICAL, PHARMACOLOGICAL AND OTHER RELATED FIELDS

Dobrushe Denburg

Date of Submission 12/06/2021

_____

Dr. Edyta M. Greer

_____

Dr. Keith Ramig

_____

Dr. Orrette Wauchope

Submitted to the Committee on Undergraduate Honors at Baruch College of the City University of New York in partial fulfillment of the requirements for the degree of Bachelor of Arts in Biology with Honors

ABSTRACT

The Computational Chemistry of Nitrogen-Rich Compounds; Insight into Pioneering Research

Nitrogen-rich functional groups have long been studied for their diversity; nitrogen can form single, double and triple bonds with itself, and will therefore exist in a very broad range of molecular arrangements. Poly-nitrogen compounds are highly energetic and electron rich, and many compounds display unique properties that allow participation in very specialized chemical reactions. However, perhaps most important is their ubiquity in biological systems, and throughout the past century and currently, their biological relevance is deeply and widely explored in biochemistry and biomedicine, from understanding their involvement in natural biological processes and complex biomolecules to the harnessing of their intrinsic properties for drug development and bioimaging.

Computational Chemistry constitutes a major area of scientific research, constantly developing since the mid 2Oth century, where the smallest components of atoms and molecules are studied through quantum mechanics, approximations and empirical data, providing energetic and geometric data to predict and elucidate their macro properties and behaviors.

Computational analysis introduces extensive applications in investigating compounds and reactions, including but not limited to; biomedical applications, including drug design and development; gaining an understanding of chemical properties where experiments fail; and predicting the interactions and reaction pathways between compounds – the feasibility and energetics of reactants, potential products and intermediates. Computational chemistry is an extremely versatile field, in that it can provide singular insight into the intricacies of an individual molecule yet extends to the behavior and arrangements of a crystal lattice, for example.

This thesis is an exploration of recent research devoted to the chemistry of azides, heterocycles, and other small nitrogen-containing molecules through quantum mechanics. Computational chemistry has emerged over the past decades as a fundamental partner in research and vital to its advancement. With selective studies, I will provide a window into the computational chemistry approach to researching these compounds; covering important heterocyclic reactions including click chemistry; the broader application of those reactions in biological systems – bioorthogonal chemistry – ; the exploration and characterization of various intrinsic and fascinating properties of heterocycles; and finally, a comprehensive look at studies of complex biomolecules that feature heterocycles in their chemical makeup. The immense range of theoretical methods available to address countless aspects and characteristics of these compounds demonstrates the tremendous value in this evolving field.

CONTENTS

1. INTRODUCTION

I RESEARCH METHODOLOGY

II INTRODUCTION TO POLY-NITROGEN COMPOUNDS

III INTRODUCTION TO COMPUTATIONAL CHEMISTRY

2. QUANTUM MECHANICS AND DENSITY FUNCTIONAL THEORY

3. PERICYCLIC AND CYCLIZATION REACTIONS, CLICK CHEMISTRY AND OTHER SYNTHESIS REACTIONS

I Electron-Rich Triazoles as Ligands in Suzuki Miyaura Cross-Coupling Reactions

DFT Calculations Performed for Frontier Molecular Orbital (FMO) and Density of State (DOS) Analyses

II CuAAC Click Chemistry Reaction for the Synthesis of Triazoles with a New Stabilizing Ligand

DFT for Global Reactivity Indices and Parr Functions

III SPAAC – Strain Promoted Azide Alkyne Cycloaddition – A Bioorthogonal Click Chemistry Reaction for Triazole Formation

A DFT Study on Reactivity and Reaction Pathway with Molecular Electron Density Theory (MEDT), Global Reactivity Indices and Parr Functionals, Intrinsic Reaction Coordinates (IRC)

IV SPAAC are Performed with Primary, Secondary and Tertiary Azides to Compare Effect on Reaction Rates and a Semi-Orthogonal Reaction is Designed

DFT Thermodynamic Calculations are used in the Bickelhaupt and Houk Activation Strain Model

V A Lactone is Successfully Utilized in 1,3-Dipolar Cycloadditions Yielding Stereospecific Triazole Derivatives

DFT Studies Reveal the Reaction Pathway and Explain the Stereoselectivity

VI Inverse Electron Demand Diels-Alder Reactions with Hydrogen Bond Donating Catalysts

Gibbs Free Energy Profiles, FMO Analysis and Electrostatic Potential Maps Reveal the Nature of the Interactions and Mechanisms

VII A Uniquely Stable Electron-Deficient Azide Displays Good Reactivity with Electron-Rich Dipolarophiles in 1,3-Dipolar Cycloaddition Reactions

DFT Reveals a Concerted, Asynchronous Mechanism Energetically Favored due to a Low Lying LUMO

VIII A Screening Process is Established for the Design of Bioorthogonal and Mutually Orthogonal Cycloaddition Reactions Using DFT Computational Analysis with the Distortion/Interaction Model

IX Isomeric Triazines Exhibit Unique Profiles of Bioorthogonal Reactivity

X The Equilibrium Ratio of Allylic Azide Rearrangement Isomers is Predicted through DFT

XI Discovering the Mechanism for the Diazonium Salt + Azide Ion Reaction Yielding Aryl Azides Using Radiolabeling

Potential Energy Surface (PES), IRC, Electrostatic Potential Maps along with Carr-Parrinello Molecular Dynamics Decode an Elusive Reaction Mechanism

XII The Design of an Azide-Migration Type Synthesis for Regioselective α-Azido Ketones

The Reaction Mechanism and Pathway is Explored with DFT

4. AZO DYES

I Heterocyclic Azo Dyes with Nitrothiazole Groups are Synthesized and Display Exceptional Color

Analysis includes TD-DFT – Time-Dependent DFT – for Electronic Absorption Spectra and DFT for Vibrational Spectra

II A Disperse Azo Dye with a Pyrazole Skeleton is Investigated Experimentally

A Complete DFT/TD-DFT Characterization with Tautomer, Conformational, Vibrational and UV-VIS Spectral Analysis and NMR

5. BIOLOGICALLY RELEVANT AND BIOLOGICALLY ACTIVE COMPOUNDS

I A Crystallographic and Electronic Analysis of a Zn(II)-Azide Complex with a N,N,S-Tridentate Thiosemicarbazone Ligand

DFT Confirmed Structural Parameters and Explained the Intermolecular Interactions Stabilizing the Crystal Structure

II Mono- *and* Bis- *Alkylated Lumazines are Synthesized as Potential Membrane-Bound Photosensitizers*[51] *Theoretical Studies with Molecular Orbital Theory and Mayr's Nucleophilic Index Provide Insight into Alkylation Patterns*

III The Debated Mechanism of Hydrolysis of Hydrazones is Clarified Through DFT Thermodynamic Calculations and a pH–Based Stability Inversion of Triazinyl Hydrazones is Examined

IV A Newly Identified Reciprocity Between Two Important Phenomena – Hydrogen Bonding and Aromaticity – in Heterocycles

V Aromaticity-Modulated Hydrogen Bonding in Biologically Important Heterocycles

VI ESPT – Excited State Proton Transfer Discovered to Relieve Excited-State Reversal of Antiaromaticity and Aromaticity

TD DFT Calculations for NCIS(1)$_{zz}$ and Energetics Calculated at S_0, S_1 and T_1 States Demonstrate this Relationship

6. AN IN-DEPTH REVIEW OF SELECTED COMPUTATIONAL INVESTIGATIONS OF IMPORTANT AND COMPLEX BIOLOGICAL AND RELATED COMPOUNDS WITH NITROGEN-CONTAINING HETEROCYCLES

I Adenine, and Purine from which it is Derived are Computationally Explored for Substituent Effect[38]

II Folic Acid Photodecomposition – DFT Investigates the Exact Nature of this Breakdown

III An Examination with DFT of the Breakdown of the Folic Acid under Hydrothermal Treatment[40]

IV Porphyrins – Fascinating Complex Molecules with a Uniquely Stable Core: An In-Depth Look at Meso-*Substituted Zinc Porphyrins and the Origins of their Special Characteristics*

V A Comprehensive Quantum Mechanical Investigation of the yet-

Inconclusive Mechanism of OH Radical Addition to Adenine – the Origins of Mutagenesis

7. CONCLUSION

8. CITATIONS

1. INTRODUCTION

I RESEARCH METHODOLOGY

Research was done in the form of an extensive, general review of relevant literature from the past decade on computational investigations of nitrogen-rich species and their properties, syntheses and reactions. Families of nitrogen compounds were systematically researched for computational-based studies, and selected works considered highly appropriate for relevance and innovation and a clear representation of the computational approach were noted as such. (Some of the compound families are described below). This research primarily included peer reviewed scientific papers accessed through the Baruch Library's 'Web of Science database.' The selected papers were subjected to an in-depth review with further research into the subjects referenced done as warranted. The information found pertinent to the thesis topic was organized and summarized and provided the basis for the thesis, provide a brief but comprehensive survey of this area in scientific research as a reference to scientists in the field.

With much appreciation to Dr. Edyta Greer for her guidance and introducing me to the world of computational chemistry through research we performed on lumazines (a heterocyclic pteridine derivative). The collaborative paper - 'Mono-and Bis-Alkylated Lumazine Sensitizers: Synthetic, Molecular Orbital Theory, Nucleophilic Index, and Photochemical Studies' was recently accepted for publication in the *Photochemistry and Photobiology* journal.[A] Dr. Greer's and Kitae Kwon's published work 'Overview of Computational Methods for Organic Chemists'[1], was an invaluable resource into the methodology and background of the computational approach.

II INTRODUCTION TO POLY-NITROGEN COMPOUNDS

Azides comprise of three nitrogen atoms in a linear arrangement, and properties arise from the nucleophilic and electrophilic nature of N1 and N3 respectively, acting as a dipolar. This allows for its ready participation in the total synthesis of many species, alkaloids are one of note, through such efficient reactions as the click-chemistry cycloaddition reactions to form other nitrogen-rich species. An example is the Huisgen reaction, a cyclization reaction of organic azides with alkynes, it is of major importance in chemical biology.[B]

Azo compounds are those that contain diazene – two nitrogen atoms with a double bond between them. They are found naturally in fungi, plants, microorganisms and some invertebrates and studies show a wide spectrum of biological activity including (primarily) anticancer, antibacterial and antiviral. More than 120 diazene-containing alkaloids have confirmed pharmacological activity, azo compounds are therefore an extremely important source in drug discovery.[B] *Diazonium salts* are a reactive diazo moiety well known for diazo coupling reactions and particularly in the formation of brightly colored (heterocyclic) azo dyes, with applications ranging from pigmentation to biomedical investigation.[C]

Triazenes are molecules containing three linearly arranged nitrogen atoms with a double bond between the first two and a single bond between the second and third. Triazenes form diverse compounds with broad applications in chemical synthesis and biomedical applications. As an example, the 1,3-diaryltriazene scaffold who's properties include antibacterial, antifungal, and efficient carbonic anhydrase inhibition

abilities.[D] Triazene compounds are pharmacologically active with limited toxicity, there are many triazene-based anti-cancer treatments and research is constantly focused on enhancing the currently available therapies and expanding the field. Dacarbazine – a triazene – is an antitumor drug which is metabolically converted into the methyl diazonium ion, which methylates DNA and successfully treats melanoma and other cancers.[E]

Pyrazoles are five-membered heterocyclic rings containing two adjacent nitrogen atoms, with one of them protonated. Pyrazoles are not commonly found in nature, but 1-pyrazolyl-alanine is a pyrazole first isolated from watermelon seeds in 1959. Pyrazoles are alkaloids, and are important scaffolds in medicinal chemistry, exhibiting much biological activity. They are present in NSAIDS, and literature lists anticancer, antiviral and neuroprotective potencies among many other areas of their biological relevance.[F]

Imidazoles are five-membered heterocyclic rings containing two nitrogen atoms, one protonated, with a carbon in between. Imidazole is a planar ring, soluble in water and basic, reactive at the protonated N site. Imidazole rings are found in many alkaloids, and they are important biological building blocks, present in histamine and the amino acid histidine for example. Histidine is vitally involved in the binding of hemoglobin, and present in many enzymes. Imidazole bound to pyrimidine forms purine, purines are building blocks of DNA and the most prevalent naturally occurring nitrogen-containing heterocycle.[G]

Triazoles are five-membered heterocyclic rings containing three nitrogen atoms. The triazole ring has been of great interest recently for its anti-cancer and free radical scavenging abilities, and research is focused on optimizing triazole derivatives.[H] The triazole's relevance is both as well-known pharmaceutically active scaffold and as a bio-isostere (a group containing similar functional properties to another that can advantageously be used in its place). They are notably stable under redox and hydrolytic conditions.[I]

Tetrazoles are five-membered heterocyclic rings containing four nitrogen atoms. Tetrazoles are involved in important synthesis reactions, a key example of which is the tetrazole-alkene 1,3 dipolar cycloaddition reaction. They can be photochemically activated, making them widely useful in bioorthogonal reactions (those that occur in living systems without interfering with native processes), for biochemical investigations.[J] Tetrazoles are present in some angiotensin II blockers, and are sometimes used in explosives due to their highly energetic properties. Tetrazoles are used in MTT assay, which is a colorimetric quantitative and sensitive detection of cell mitochondrial activity growth rate.[K]

Triazines are six-membered heterocycles with three nitrogen atoms, they are highly reactive and easily modified and have many uses in agriculture and medicine. The 1,3,5-triazine is an important privileged structure and a most recent focus in rational drug design and development has been in creating triazine-based hybrids, harnessing the triazines' inherent potencies as well as that of various functional groups in providing multi-targeted therapies for challenging diseases including cancer, neurodegeneration and parasitic infections.[L] Triazines are the basis of many herbicides, fungicides, and insecticides.[M]

Tetrazines are six-membered heterocycles with four nitrogen atoms. Tetrazines are frequently used in bioorthogonal reactions, recently as a powerful tool in medical imaging and diagnostics, for example in tetrazine-functionalized dyes or 'fluorogenic probes.' The reactive ring is easily modified and has good pharmacokinetic abilities making it an ideal candidate for expansion of its bioorthogonal capabilities.[N]

III INTRODUCTION TO THE COMPUTATIONAL CHEMISTRY APPROACH

Computational analyses are often employed to provide elucidation of the mechanisms of chemical reactions, especially those difficult or impossible to observe experimentally. They are used to verify or confirm experiments, and at times replace them all together once experimental investigation has reached its limits. They are effective in drug design, in understanding pharmaceutically important molecules on a molecular level: Computations can incomparably build an intuition not achievable when approaching the bulk, by providing insight into the individual molecule, how the groups within it interact and relate, whether those interactions are stabilizing or destabilizing and how those patterns affect the molecule as whole. Computational analysis can in turn explicate material and crystal properties and behavior, this versatility extending to simulations of phenomena, like weather for example.

Quantum calculations are used to understand molecules' geometry and behavior in ground and excited states. Different methods and basis sets are used selectively to optimize structures, look at molecular orbitals, electrophilicity, nucleophilicity, charge distribution and spin density. These methods assess the stabilities, energies and vibrational frequencies of reactants, intermediates (transition states) and products, determine energy barriers to reaction pathways, provide solvent and gas phase simulations, providing insight into the dynamics of molecular collisions.

Ab initio methods are based on quantum chemistry, but also include approximations, for example *Hartree-Fock,* which provides a simplification of the *Schrödinger Equation* for wave function – only the wave function of H and H_2^+ can be exactly determined. *Ab initio* calculations provide thermodynamics, energetics and electron density.[1]

Density Functional Theory (DFT) is based on the energy of a molecule being a function of electron density: where the probability of any number of electrons occupying a unit volume in space can be imagined as 'electron gas'. There are multiple DFT functionals including B3LYP.[1]

Semi-Empirical Methods have a basis in Molecular Orbital theory – valence electrons are viewed as influenced by the entire molecule rather than individual nuclei – and use experimental results to supplement an absence of calculated integrals, these methods are much faster than *ab initio* methods but are not as precise.[1]

2. QUANTUM MECHANICS AND DENSITY FUNCTIONAL THEORY

DFT – Density Functional Theory is a quantum mechanics-based modelling system for chemical structure and reactivity as a function of electron density – the number of electrons in a given unit of space – the energy of a particle is described as a function of electron density, and at ground state, this functional is at a global minimum.[1]

Quantum theory calculations began with Hartree-Fock – HF – based on computationally expensive *ab initio* methods which are a many-electron-function approach to predicting molecular interactions based solely on fundamental physical constants.[1] (The HF method was an extension of the Hartree method, satisfying the Pauli exclusion principal that states that two electrons cannot occupy the same quantum state, they must have anti parallel spin).[2] The HF method uses approximations to determine the wavefunction and energy of a (stationary) many-electron quantum system – it is an approximation to the solution of the Schrödinger's equation {that predicts the behavior of an electron}, for the system.[2] HF theory does not account for electron repulsion and the impact of electrons' movement within a system on each other. Based on HF, Gaussian functions were developed for mathematically computing stationary wave functions and energy for atoms and molecules at a desired accuracy.[1,2] Gaussian basis sets are sets of one-electron functions that are linearly combined to form molecular orbitals.[1]

Hohenberg and Kohn first proposed that ground state energy can be described as a function of ground state *electron density* – this is the basis of DFT – and in this vein the Kohn-Sham equation approximates the (single-electron) Schrödinger's equation, that describes the wave function of a *quantum system* as well as electron-correlation effects. Kohn and Sham described the energy as a combination of kinetic, potential, Coulomb and correlation energy.[1] They considered the electron density of the system as non-interacting and each lowest energy orbital is incorporated in the Kohn-Sham wavefunction – a single Slater determinant (description of a fermion {subatomic particle} wavefunction) – along with an approximation of electron exchange and correlation, yet calculated at the local (one-electron) level. This correlation approximation therefor remains somewhat limited in describing highly varying electron density and lower electron density – further from nuclei, particularly where atoms' orbitals overlap in a molecule, at the 'surface.' [1,3] DFT uses a variety of functionals, including hybrid functionals that combine DFT and HF, for example the B3LYP function – named for Becke who introduced this *combined* DFT and HF (exact exchange) approach – with Lee, Yang and Parr's correlation functional, this approach appropriately handling molecular properties.[1] Basis sets in general are selected according to characteristics of the molecule or system at hand.[1]

3. PERICYCLIC AND CYCLIZATION REACTIONS, CLICK CHEMISTRY AND OTHER SYNTHESIS REACTIONS

I Electron-Rich Triazoles as Ligands in Suzuki Miyaura Cross-Coupling Reactions

DFT Calculations Performed for Frontier Molecular Orbital (FMO) and Density of State (DOS) Analyses

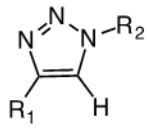

Click-synthesized triazole ligands, R_1 = 2-OMePh/2,6-OMePh/phenyl and R_2 = 4-OMePh/phenyl

A series of triazole ligands were synthesized for enhanced catalysis of the Suzuki Miyaura cross-coupling reaction of aryl halides, which are relatively unreactive.[4] The tetrakis(triphenylphosphine)palladium, $Pd(PPh_3)_4$-catalyzed coupling reaction was developed by Suzuki and Miyaura in 1981, who reported an unprecedentedly high yield of biaryls through the coupling of phenyl-boronic acid with haloarenes in a relatively simple reaction.[5] In 2010, Akira Suzuki was a joint winner in The Nobel Prize in Chemistry awarded 'for palladium-catalyzed cross couplings in organic synthesis,' and this reaction is considered the most important method for synthesizing biaryls and their derivatives – very important compounds found throughout nature and pharmaceuticals – a good example is in the synthesis of the powerful antibiotic vancomycin.[6]

The Suzuki Miyaura cross-coupling reaction involves the formation of a C – C bond by way of a halide and organoboron coupling, catalyzed by a palladium complex and a base. The Pd complex catalyzes the first step of the cross-coupling reaction, the oxidative addition of the Pd to the halide – $[R_1 – Pd – X]$ – and the success of this is predicated upon the ligands' electronic properties. The addition is followed by transmetallation with the boronate group (formed from the base interaction with boronic acid) which gives $[R_1 – Pd – R_2]$, then followed by reductive elimination for the coupled organic product and the regenerated catalyst. This final step is again affected by the electronic as well as steric properties of the ligand. Electron-rich ligands will enhance reactivity, and so ligands with the electron rich triazole heterocycle are designed and studied for their catalytic activity. Given the multiple catalysis steps, efficient design of these reactions is complex, and so theoretical calculations are engaged to assist.[4]

B3LYP with the 6-31G (d, p) basis set was employed for the calculations of optimized geometries, FMO energy calculations and diagrams, and for DOS calculations, in order to study the different proposed triazole ligands' structure and geometry, and their coordination to the Pd core of the ligand-metal complex. FMO – Frontier Molecular Orbital – theory looks at HOMO – Highest Occupied Molecular Orbital – and LUMO – Lowest Unoccupied Molecular Orbitals – where electronic density directs the electrochemical (and photochemical) properties of the molecule. Electron density in the HOMO represents a nucleophilic region; whereas the LUMO is electrophilic. Reactivity is predicated upon the gap between these two energy levels; a small gap, often denoted as 'chemical softness,' represents an easy transition to the excited state and therefore a reactive species; a large gap or 'chemical hardness' a more stable, less polarizable molecule.[4]

FMO analysis – calculated energy gaps – of the ligands showed an electron-rich triazole core (HOMO), further stabilized by electron density from the other electron (-rich) donating groups of the molecule; allowing it to form a complex with Pd. DOS – Density of State – refers to the number of states available for

occupation by an electron at each energy level – was computed for electron distribution patterns, and was used to back up the FMO analysis.[4]

Experimental results and computational predictions were in good agreement in their findings that the 4-(2,6-dimethoxyphenyl)-1-phenyl-1H-1,2,3-triazole ligand, electron dense and sterically bulky, was an efficient ligand in the cross-coupling reaction, providing a very high level of reactivity for the generally unreactive aryl-chloride.[4]

II CuAAC Click Chemistry Reaction for the Synthesis of Triazoles with a New Stabilizing Ligand[7]

DFT for Global Reactivity Indices and Parr Functions[7]

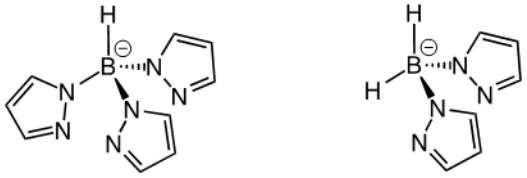

Tris(pyrazolyl)hydroborate $HB(pz)_3^-$ and bis(pyrazolyl)hydroborate $H2B(pz)_2^-$ stabilizing ligands

Certain synthesis reactions that adhere to strict standards of high stereospecific yield, room temperature conditions, environmentally benign solvents and easily isolatable by-products are referred to as 'click chemistry.' Many cycloadditions reactions well represent click chemistry ideals, and predominantly involve the formation of C – heteroatom bonds and are considered the preeminent synthesis methods for complex biological and chemical molecules, giving rise to a huge variety of five and six membered heterocycles.[8] CuAAC – copper(I)-catalyzed azide-alkyne cycloaddition – is a click 3+2 cycloaddition – 32CA – reaction that yields 1,2,3-triazoles. Triazoles are highly important bioisosteres – a molecule where functional groups or atoms are replaced with relatively similar moieties allowing it to retain only its desired biological properties.[7] The advantageous CuAAC reaction is still potentially complicated by the instability of Cu(I) that can easily oxidize to Cu(II) in aerobic conditions, so an experimental and computational study is performed on two poly(pyrazolyl)borate anions – tris(pyrazolyl)hydroborate $HB(pz)_3^-$ and bis(pyrazolyl)hydroborate $H2B(pz)_2^-$– which are successfully employed as novel stabilizing ligands in a copper(I) complex to catalyze the formation of complex triazoles, including those containing sugar groups, and therefore biologically relevant.

Experimentally, poly(pyrazolyl)borates were screened with a series of click-conforming solvents to determine the optimal conditions, and then with a series of azide and alkyne derivatives, a representative reaction resulted in 95% yield of the disubstituted triazole after 24 hours in ideal conditions. Computations optimized the structures of these coordination complexes and assessed the reactivity of the acetylide intermediates and predicted a reaction pathway.[7] DFT calculations were performed at the B3LYP/6-31G(d) level for optimized geometries of reactants and intermediates – including both the simplest Cu(I) complex intermediate, dinuclear copper(I)-acetylide, and the dinuclear (bis(pyrazolyl)borate)-Cu(I)-acetylide.[7] The optimized structures were assessed for reactivity by looking at their global reactivity indices; including global electrophilicity – ω – the ability to attract electrons; global nucleophilicity – N – donating electrons; chemical hardness – η –, where reactivity is based on the difference in energy levels of the frontier molecular orbitals; and chemical potential – μ.[7]

In contrast to the basic Cu(I) intermediate, for which the indices did not predict a polar 3+2 CA, the poly(pyrazolyl)borate-stabilized complex displayed a diminished ω and elevated N, characterizing it as a strong nucleophile and therefore beneficial in a polar 32CA reaction. Parr functions – Pk^+ and Pk^- – are used to predict reactivity in polar reactions, and are a local measure of excess spin-electron density or spin polarization, associated with GEDT – global electron density transfer – between the nucleophilic and electrophilic centers;[8] these calculations enabled the proposal of a regioselective mechanism for the cycloaddition.[7]

Both experimental and computational results supported the superior catalytic capabilities of the poly(pyrazolyl)borate-copper(I) in the subject CuAAC reaction, a result of its enhancing of the polarity-driven cycloaddition reaction with its highly nucleophilic character. This 32CA reaction displayed compatibility with many complex substituent groups, including sugar moieties, with potential biological relevance.

III SPAAC – Strain Promoted Azide Alkyne Cycloaddition – A Bioorthogonal Click Chemistry Reaction for Triazole Formation[10]

A DFT Study on Reactivity and Reaction Pathway with Molecular Electron Density Theory (MEDT), Global Reactivity Indices and Parr Functionals, Intrinsic Reaction Coordinates (IRC)[10]

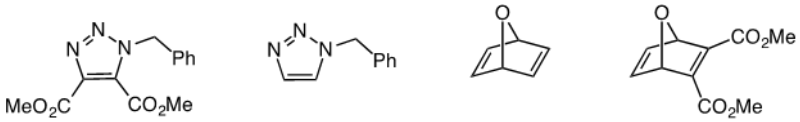

SPAAC click-synthesized triazoles; OND; DMAD

Azides can be introduced into living cells as reporters, detectable through cycloaddition reactions. Standard cycloaddition reactions are often catalyzed by metal complexes toxic to the human body and therefore much research has been invested in developing SPAAC – strain promoted azide alkyne cycloaddition – reactions that are catalyst free and operate under physiological conditions.[10]

The tandem 32CA/retro Diels-Alder of OND (oxanobornadienedicarboxylate) and benzyl azide has recently been developed as a bioorthogonal click reaction that produces the triazole product, and at a faster rate than the strain-free DMAD (dimethyl acetylenedicarboxylate) and azide reaction with a similar product. Bioorthogonal chemistry involves reactions that can be introduced into biological systems that don't otherwise participate in or affect native processes, a reporter is introduced and incorporated into a target, followed by the addition of a fluorescent-labeled probe that will bond covalently with the reporter, subsequent imaging can now locate the target molecule.[11] A retro Diels-Alder reaction is the formation of a diene and dienophile from cyclohexene – the reverse of the DA cycloaddition reaction.

Computational calculations, at two different levels of theory – B3LYP/6-31G (d,p) and M06-2X/6-31G (d,p) – have been used to investigate the relationship between structure, mechanism and reactivity in these reactions. M06 or Minnesota functionals are DFT methods based on spin densities, M06-2X incorporates Hartree-Fock theory as well and is well suited to looking at noncovalent interactions and thermodynamic parameters of non-metals.[1]

A series of parameters were employed to provide insight into how the reaction progresses. MEDT – molecular electron density theory – describes reactivity as a function of changes in electron density and the associated energetics along the reaction pathway. Global indices (η, μ, ω, N) and Parr functions were calculated for OND, DMAD and benzyl azide, the global indices showed a big gap in electrophilicity between OND and benzyl azide indicating its influence on the direction of electron density transfer in the reaction.[10] GEDT calculates the polarity of reactions based on the transfer of electron density at the transition states (TSs), and it indicated only one polar retro-DA TS, the other reaction pathways being non-polar. Regioselectivity is predicted by Parr functions and was used to identify the favored triazole. HSAB – hard and soft acid and base – principal also looks at regioselectivity based on the local softness S+ and S- of the interacting atoms, with the favorable reaction between those of similar softness.[10] Gibbs free energy calculations at all stationary points were employed to determine the favored reaction pathway for the domino reaction. The Berny method was used to optimize the transition states, whereas calculated frequencies ascertained only one imaginary frequency (per TS). IRC – intrinsic reaction coordinate – pathways are traced for a look at energy profiles and to connect TSs to energy minima. ELF – electron localization function – analysis for monosynaptic and disynaptic basins for lone pairs and bonding regions, respectively, and the changes in bonding throughout the reaction give deeper mechanistic insight, as does NCI – noncovalent interactions index – which analyzes attractive and repulsive interactions.

This in-depth computational expedition along the reaction pathways depicts an OND/methyl azide CA/RDA reaction with lower activation energy than the DMAD, and describes the favored pathway, both aspects in good agreement with experimental results.

IV SPAAC Performed with Primary, Secondary and Tertiary Azides to Compare Effect on Reaction Rates and a Semi-Orthogonal Reaction is Designed [12]

DFT Thermodynamic Calculations are used in the Bickelhaupt and Houk Activation Strain Model [12]

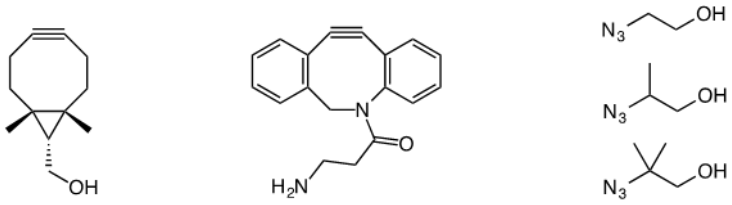

BCN; ADIBO; primary, secondary and tertiary azides

SPAAC reactions are among the most ubiquitous biorthogonal reactions.[12] It is a 1,3-dipolar cycloaddition between a cyclooctyne and an organic azide for the very stable triazole linkage, the rate of reaction is driven by the distortion of the cycloalkyne. Azides are used advantageously because of their bioorthogonality, small size and high stability, they can be metabolically incorporated into biological molecules.[12] SPAAC reactions are spontaneous at room temperature and much research has been focused on the alkyne component to improve kinetics. Here, a series of primary, secondary and tertiary azides are investigated for their relative effect on reaction rates with two commonly used cyclooctynes – BCN and ADIBO. It was hypothesized that the bulky tertiary azides would exhibit low reactivity with the sterically demanding ADIBO and experimental results, expectedly, showed a rate decrease of several orders of magnitude. With the

non-sterically demanding BCN, there were similar reaction rates for all azide species. This chemo-selective behavior can potentially be exploited for catalyst-free semi-orthogonal dual-labeling (where at least one reactant pair will interact independently of the second set of reactants) with SPAAC. [12]

The low 3° azide/ADIBO reactivity was explored by DFT using B3LYP-D3 with the 6-311+G(d,p) basis set – it was used for structure optimization and energetics, including that of transition states, Gibbs free energies of activation, and reaction rates. The Bickelhaupt and Houk activation strain model {this will be explained further} was applied: briefly, it is based on the strain energy for distortion to transition state geometry – ΔE_{strain} – and the energy associated with the interaction (formation of new bonds) – ΔE_{int}. These analyses were graphed and the interaction energy was further broken down into the following components using B3LYPD3/TZ2P//B3LYPD3/6-311+G(d,p): ΔV_{elstat}, for classic electrostatic forces; ΔE_{Pauli}, for closed shell repulsion and sterics; ΔE_{oi} for charge transfer between FMOs and polarization; and ΔE_{disp} for dispersion forces. This analysis highlighted that the difference in reactivity of the 3° azide resides primarily in sterics – ΔE_{Pauli}. [12]

With this explained, experimental research was expanded into dual labeling and successfully employed a 1° azide/3° azide – ADIBO/BCN combination that was reliably semiorthogonal when the 3° azide was added following the 1°. The dual labelled product was yielded in excess of 99%. [12]

V A Lactone is Successfully Utilized in 1,3-Dipolar Cycloadditions Yielding Stereospecific Triazole Derivatives[13]

DFT Studies Reveal the Reaction Pathway and Explain the Stereoselectivity[13]

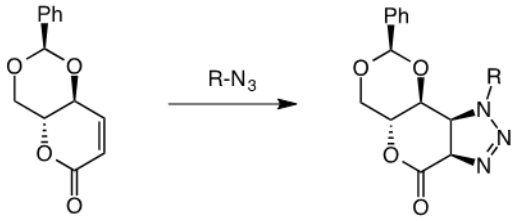

Stereoselective lactone D-erythrose 1,3-dioxane; triazoline lactone derivative - the stereospecific cycloaddition product

D-erythrose 1,3-dioxane has previously been synthesized and characterized as a highly stereoselective dipolarophile thar will react with a 1,3-dipole to form a five-membered heterocycle.[13] Synthesized from readily available D-glucose, tetroses (four-carbon sugars) in general, are very valuable in the synthesis of large molecules with multiple chiral centers, through Wittig elongation of the aldehyde group. However, poor facial selectivity due to the double bond's high degree of freedom has limited these tetroses' usefulness.[13] Stereoselectivity involves which 'face' of the lactone reacts with the dipole. Regioselectivity with a non-symmetrical dipole involves the potential formation of two regioisomers based on the orientation of the approaching dipole, regioselectivity is the preference of chemical bonding or breaking in one direction over all other possible directions. The lactone contains its double bond within a ring, improving the stereoselectivity as well as increasing reactivity and is therefore potentially a good 1,4-Michael acceptor (for 1,4 addition reactions with resonance-stabilized carbon nucleophiles), and electron-deficient dipolarophile. {3+2} cycloaddition reactions of the lactone with alkyl azides and phenyldiazomethane were performed and experimental triazoline yields were moderate to high, and

importantly, all with complete regio- and sterio- selectivity – for each reaction only one product was formed.[13]

DFT studies focused on the energetic pathways as a means to understand the experimental results. The reactions can proceed in concerted or stepwise fashion; with polar, nonpolar or diradical character. Geometry optimization and atomic charge distribution was performed at the B3LYP 6-31G(d) level with the PCM – polarizable continuum model – to account for solvent effects. A search was performed for transition states, which were then fully optimized. IRC calculations were performed, and the products and reactants were connected to the transition states. Energies were all computed at the M06-2X 6-311++G(3df,2dp) level with IEF-PCM.[13]

For all three cycloadditions, the computations revealed a concerted formation of two covalent bonds between the dipole and the lactone, with highly ordered transition states, directed by sterics and electronic interactions. In all cases, the cycloadditions (nucleophilic attack) occurred at the *re* face of the lactone ring: the transition state structures showed the keto groups perpendicular to the new 1,3-dipole bonds, due to H atoms at the *si* face that inhibits correct alignment of the dipole as well as a hyperconjugative effect of the C – O bond of the lactone on the positive end of the dipole. Calculated free energies of activation supported this approach.[13]

The regioselectivity was examined by FMO theory, where the favored reaction is the complementary interaction between the molecules' frontier orbitals – for which there are three possibilities: a dipole HOMO and dipolarophile LUMO; in the case of similar ΔE, both HOMO-LUMO interactions are important; and, dipole LUMO and dipolarophile HOMO. FMO analysis of the TSs revealed that the diazo reaction was of the first type, whereas the azide reactions were of the second variety, common for a strong nucleophile.[13]

To understand the appearance of only one regioisomer, profiles for free energies of activation and interaction for the cycloadditions – these reactions are governed by highly ordered transition states – showed the thermodynamically favored pathway for each. The activation energies were decomposed into distortion, entropic, interaction and solvent effects, depicting the distortion energy as the main contributor; with the difference in distortion energies along the pathways revealing the favored regioisomer where less distortion of the dipole is required.[13]

The synthesized lactone was found to be highly selective and high yielding in the cycloaddition reactions for complex triazoline derivatives with multiple chiral centers. The DFT approach explained these results, revealing a concerted mechanism and a regioselective process, where, of the two possible pathways to cycloaddition based on the dipoles' orientation, the lower distortion-demanding path is favored.[13]

VI Inverse Electron Demand Diels-Alder Reactions with Hydrogen Bond Donating Catalysts[14]

Gibbs Free Energy Profiles, FMO Analysis and Electrostatic Potential Maps Reveal the Nature of the Interactions and Mechanisms[14]

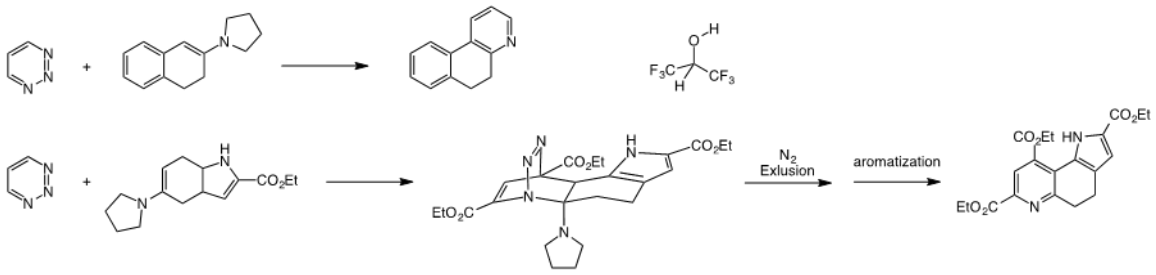

1,2,3-triazine and enamine cycloaddition reaction; HFIP; the Diels-Alder reaction scheme

The IED-DA – Inverse Electron Demand Diels–Alder – reaction is an organic chemical reaction, in which two new chemical bonds and a six-membered heterocycle are formed. These reactions have long been recognized for their value in bioorthogonal chemistry and research has demonstrated their powerful synthetic ability in the total product synthesis of very highly complex natural products that range from potent anti-tumor and anti-cancer agents to LSD and allow for the integration of specific features of natural products into biologically active molecules.[15] The IED-DA is related to the Diels–Alder reaction but differs in that it is a cycloaddition between an electron-poor diene and an electron-rich dienophile. During an IED-DA reaction, three π bonds are broken, and two σ bonds and one new π bond are formed. IED-DA reactions between unsubstituted and substituted 1,2,3-triazines and enamine were studied computationally to look at substituent and solvent – in particular HFIP (hexafluoroisopropanol), recently found to accelerate the 1,2,3-triazine cycloaddition through hydrogen bond donation – effects on reactivity and mechanism. Generally, the cycloaddition is predicted to occur in a concerted manner (involving the concerted, asynchronous formation of the cycloadduct, followed by a rapid N_2 release and then aromatization).[14]

DFT was performed at M06-2X 6-31G(d,p) for geometry optimizations and vibrational frequencies to confirm TSs and that optimized structures are energy minima. Single-point energy calculations were performed on these optimized structures of the reactants, TSs, intermediates (including HFIP-triazine complexes and DA adducts) and products at the M06-2X 6-311+G(d,p) with the CPCM for HFIP and $CHCl_3$, as well as with an explicit HFIP molecule, to construct Gibbs free energy profiles with *exo/endo* energetic pathways for the series of reactions.[14]

The parent triazine showed an asynchronous concerted mechanism without the catalyst. With HFIP, the reaction proceeds stepwise with a H-bond-stabilized zwitterionic intermediate (structure optimizations depict shorter H-bond distances on the zwitterions) and a lowered energy barrier.[14]

A CO_2Et (electron withdrawing) di-substituted triazine showed a stepwise mechanism with shallow zwitterionic intermediates on the Potential Energy Surface, with the C – C bond forming before the C – N, in both uncatalyzed and HFIP catalyzed processes. ESP – electrostatic potential – maps depict the charge separation on the zwitterionic intermediates, and where HFIP is present, the charge separation is significantly enhanced. HFIP lowers the activation barrier for a 10^4 increase in reaction rate.[14] FMO calculations on the enamine, triazines and HFIP-triazine complexes revealed that the H-bonding lowered the LUMO+1, as did the EWGs. The decreased HOMO-LUMO ΔEs were in correlation with the DA reaction barriers.[14]

DFT has illuminated the effects of electron withdrawing groups and the hydrogen-bond donating HFIP in these IED-DA reactions, in their stabilization of zwitterionic intermediates that leads to stepwise mechanisms and decreased energy barriers.

VII A Uniquely Stable Electron-Deficient Azide Displays Good Reactivity with Electron-Rich Dipolarophiles in 1,3-Dipolar Cycloaddition Reactions[16]

DFT Reveals a Concerted, Asynchronous Mechanism Energetically Favored due to a Low Lying LUMO[16]

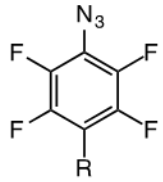

PFAA - perfluoroarylazide

Organic azides are incredibly versatile – resonance stabilized, they are physiologically inert, while their small size lends to extensive biological application. They participate extensively and reliably in cycloaddition reactions for material functionalization and bioorthogonal chemistry.[16] Azides are ambiphilic – meaning both HOMO and LUMO controlled – but somewhat non-reactive given their stability. The introduction of EWGs (electron withdrawing groups) boosts reactivity but destabilizes the compounds at room temperature. The subject electron-deficient azide – PFAA (perfluoroarylazide) – is uniquely thermally stable and compatible with biological conditions and has been used for functionalization chemistry – where functional groups are added for surface properties – and for photoaffinity – for the covalent labeling of proteins in situ.[16]

Here, PFAAs are studied experimentally and computationally for 1,3-dipolar cycloaddition capabilities, potentially expanding the compounds' chemistry. The perfluorination is understood to lower PFAAs' LUMO thereby enhancing their reactivity with electron-rich dipolarophiles. A series of PFAAs are reacted with various enamines and compared to simple phenyl azide cycloadditions, rates were greater by almost 10^4 compared to the phenyl azide, and computations explored the origins of this increased reactivity.[16]

Structure optimization was performed at the M06-2X 6-31G(d) level using an ultrafine grid, for reactants, transition states and products. Energetics were calculated for the transition state structures at M06-2X/6-311+G(d,p)/IEFPCM CHCl3 //M06-2X/6-31G(d). IEFPCM and showed concerted, asynchronous geometries as evidenced by the differing forming-bond lengths (previous research has determined a concerted, asynchronous mechanism which was confirmed by calculating the free energies associated with both stepwise and concerted mechanisms, the latter coming in decisively lower).[16] This asynchronicity is due to the interaction of the high-lying $HOMO_{enamine}$ with $LUMO_{azide}$. With increasing electron-deficiency, lower activation energies were required, and the distortion/interaction model was used to explore differences in reactivity.[16] The activation energy is based on the difference between the distortion and interaction energy; the distortion energy required of both azide and enamine to achieve the transition state geometry; and the interaction energy – effectively the net stabilizing energy – due to stabilizing orbital interactions. FMO analysis at HF/6-31G(d)//M06-2X/6-31G(d)/IEF-PCM$CHCl_3$ confirmed that the perfluorination of the aryl

ring results in the lowered $LUMO_{azide}$ and resultant smaller energy gap between it and $HOMO_{enamine}$ for greater orbital interaction.[16]

DFT elucidated the advantages of PFAAs that are most successfully exploited in their reactions with enamines; and lie in the smaller $LUMO_{azide}$ – $HOMO_{enamine}$ ΔG, the lower lying LUMO a product of the perfluorination of the aryl azide.

VIII A Screening Process is Established for the Design of Bioorthogonal and Mutually Orthogonal Cycloaddition Reactions Using DFT Computational Analysis with the Distortion/Interaction Model[17]

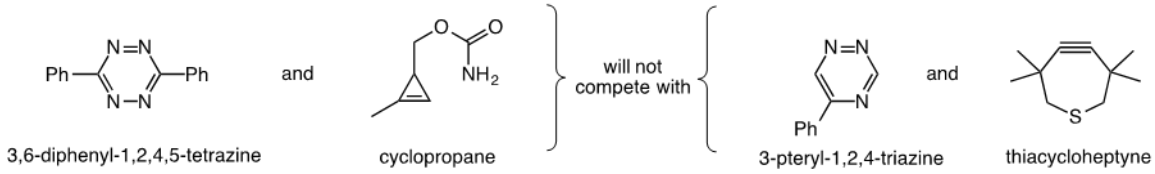

3,6-diphenyl-1,2,4,5-tetrazine | cyclopropane | 3-pteryl-1,2,4-triazine | thiacycloheptyne

Mutually orthogonal bioorthogonal reactions

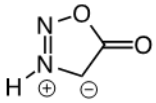

Sydnone – a meso-ionic dipolar with charges delocalized across the ring but non-aromatic

Cycloaddition reactions dominate the field of the organic synthesis of heterocycles – prevalent in drugs and natural products – and is vital in chemical biology and drug discovery. The most common cycloaddition reactions are the Diels-Alder reaction and the 1,3 dipolar cycloaddition.[17]

In a much earlier study of the 1,3-dipolar cycloaddition reaction, authors of this study performed computations, with the CBS-QB3 method, on a series of cycloaddition reactions composed of derivatives of three important dipoles, each one reacted with ethylene and acetylene.[18] The calculated $\Delta H_{transition}$ state and $\Delta H_{reaction}$ displayed a surprisingly linear relationship in most cases, with two of the classes also bearing almost identical activation barrier heights, despite displaying very different reactivity based on HOMO/LUMO ground state energy gaps. Exploring an idea recently suggested that barrier heights are influenced by distortion energies in cycloadditions, B3LYP calculations were performed for total $\Delta E_{distortion}$ for the TS of both the dipole and dipolarophiles, essentially the energy required for each to distort to TS geometry without any interaction between reactants. Results displayed a remarkably direct correlation between the $\Delta E_{distortion}$ and the activation barriers.[18] This linear correlation led to our authors' proposal of the distortion/interaction model, where activation energy is the sum total of the distortion energies to achieve concerted TS geometry – where the overlap of (FMO) orbitals of the distorted reactants is greatest – and the $\Delta E_{interaction}$, the charge transfer that overcomes the destabilization of the distortion.[19]

The D/I model was successfully expanded to quantitate reactivity and selectivity origins and has been successfully applied to organometallic and nucleophilic addition reactions as well. Most recently, to investigate mutual orthogonality in bioorthogonal cycloadditions, a very important current research focus.

In bioorthogonal labeling, a reporter is introduced and incorporated into a target, followed by the addition of a fluorescent-labeled probe that will bond covalently with the reporter, subsequent imaging can now

locate the target molecule.[20] This system was pioneered by Bertozzi, the perhaps earliest reaction involved identifying proteins with glycosylated Serine and Threonine amino acid residues in vitro, by creating analogues tolerated by the enzyme that catalyzes the glycolysation. These analogues, bearing an azido sugar, are then metabolically incorporated into cytoplasmic and nuclear proteins. In turn, biochemical probes can be introduced that will covalently bind with these O-GlcNAc modified proteins, identifying the proteins themselves and the residues that were modified.[20] The pool of bioorthogonal reactions has since expanded, taking advantage of the Staudinger ligation, SPAAC, CuAAC and tetrazine ligation. From low to high, rates of reaction for these processes are categorized as; too slow for bioorthogonal application; sufficient for labeling; to suitable for in-vivo chemistry and the tracking of metabolic processes. Mutually orthogonal (reporter and probe) reaction pairs are of particular value, allowing dual labeling.[17]

The D/I model is employed along the potential energy surface of the reaction. At the transition state, the energy requirement of the reactants to reach the distorted geometry is counteracted by the stabilizing interaction energy, the difference between the two is the activation energy.[17]

DFT calculations are performed at M06-2X 6-31G(d), with solvent effects (water) evaluated at M06-2X 6-311+G(d,p) with SCRF using CPCM on the gas phase optimizations. Computed and experimental free energies of activation were in good agreement.[17]D/I analysis was performed on biarylazacyclootynone, known to react rapidly with azides. A series of derivatives of this dipolarophiles were reacted with benzyl azides with D/I analysis successful in explaining reactivities observed.[17]

The model was also employed to investigate the cycloadditions of transcyclooctene with tetrazines, and dibenzocyclooctynes with azides, these two reactions are mutually orthogonal (they do not interfere with each other) bioorthogonal reactions and were used in tandem to label two different cancer cell types.[17] The tetrazine reactions in all cases had significantly more favorable interaction energies, which FMO analysis attributed to its low lying LUMO, but the enhanced distortion energy requirement in the dibenzocylooctyne reaction due to steric effect drastically lowered the reaction rate, with the azide exclusively reacting with this dipolarophile. This steric effect was now considered in reactivity forecast for bioorthogonal tetrazine chemistry, and further to this, triazine cycloadditions.[17]

Drawing on the success of this model, bioorthogonal reactions of the relatively recently synthesized sydnone – a *meso*-ionic dipolar with charges delocalized across the ring but non-aromatic – was discovered, computationally-guided; a screening process was developed and applied to predict a high reactivity between these compounds and dibenzocyclooctynes, two mutually orthogonal reactions employing the sydnone cycloadditions were proposed and were subsequently experimentally confirmed.[17]

Given the endless possible combinations, this model is now being used systematically by the authors to calculate second order rate constants in water at room temperature for the 1,3 dipolar cycloadditions of dipoles/dienes and dipolarophiles/dienophiles (known biorthogonal compounds). The results have been compiled into a color-coded matrix that serves as a reference to enable the direct identification of mutually orthogonal reactions.[17]

Researchers systematically looked through a collection of dipoles, dienes, dipolarophiles and dienophiles, computing their cycloaddition (IED Diels–Alder) reaction rate constants (using experimental results of some established reactant sets as a baseline for comparison) with the intention of looking for new biorthogonal pairs, as well as mutually orthogonal pairs as potential new biological reporters and trackers. Using the distortion/interaction model which is based on the energy required to distort the reactants into transition

state geometries (activation strain), which is then overcome with the interaction energy associated with the new bonds forming. The series of reactants (and reactions) were charted and color-coded based on second order reaction rates as an accessible guide to orthogonality.[17]

IX Isomeric Triazines Exhibit Unique Profiles of Bioorthogonal Reactivity[21]

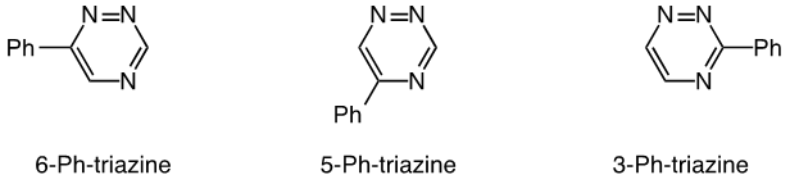

6-Ph-triazine 5-Ph-triazine 3-Ph-triazine

Isomeric triazines

The authors most recently report an expanded analysis of 1,2,4-triazines as a bioorthogonal agent, pursuant to a six-substituted derivative that has been identified as a new privileged scaffold, undergoing IED-DA cycloadditions (a [4+2] cycloaddition, in which one reactant molecule contributes four π electrons and the other two π electrons to the newly formed bonds) with TCO (*trans*-cyclooctyne) while remaining inert to biological processes.[21]

While tetrazines were considered the standard in IED-DA, undergoing robust activity with various strained dienophiles, they are also unstable in vivo and quite liable to undergo side reactions. Triazines are known for their stability in biological conditions and thus their reactivity with dienes, relative to tetrazines', was explored computationally.[21] M06-2X/6-311+G(d,p)//M06-2X/6-31G with CPCM for water, was engaged for free energies of activation, and FMO analysis was performed with HF/6-311+G(d,p)//M06-2X/6-31G(d) given that inverse electron demand reactivity is predicated upon the interaction of the diene's π* (LUMO+1) orbital with the HOMO of the dienophile.[21] Calculations showed that the 1,2,4-triazine was significantly more reactive that 1,2,3-triazines, but less reactive than the (extremely fast TCO reaction with) tetrazines – a product of the triazines' lowered LUMO. However, given their inertness to side reactions – also determined with DFT – and small size, their potential as a bioorthogonal IED-DA candidate – as a privileged scaffold – was affirmed.[22]

Drawing on this, the authors sought to examine reactivities of differently substituted 1,2,4-triazines, and possibly exploit their regioselectivity to develop new mutually orthogonal reactions, where a substitution at the six vs five on the ring would exclude reactivity with a sterically encumbered dienophile.[21] For a look at their reactivity across a range of dienophiles, triazines and tetrazines were modeled by placing phenyl groups at varying sites and DFT was employed to predict second order rate constants in water at room temperature, using M06-2X/6-311+G(d,p)//M06-2X/6-31G(d). Interactions with strained alkenes were limited to tetrazines (as expected, with lower LUMO+1 energies) besides, singularly, the 6-substituted triazine and TCO. Closer focus was applied to the strained alkynes, specifically the sterically encumbered cycloalkyne, TMTH (tetramethylthiacycloheptyne). Calculations revealed that steric clashes precluded the reactivity of all but the 5-substituted 1,2,4-triazine, and that none of the triazines would react with other alkynes: a reaction exploitable for orthogonal chemistry.[21] An experimental investigation was performed, with calculated reactions rates a close match to DFT predictions. 6-phenyl-1,2,4-triazine showed decent reactivity with TCO, and 5-phenyl-1,2,4-triazine displayed robust reactivity with TMTH, the particular reactivity profile of the latter lending itself to immediate application. Distortion/interaction analysis was

applied to demonstrate the origins of the mutual orthogonality of the reactions in this study: When considering a sterically unencumbered dienophile, the lower LUMO+1 energy of the tetrazine provides a far more stabilizing interaction energy strongly favoring this reaction. When considering a bulky alkyne dienophile, a much more energetically demanding distortion of the sterically hindered tetrazine results in an elevated activation energy, making this reaction unlikely, whereas the 5-phenyl-1,2,4-triazine has a very low activation barrier.[21]

These two cycloadditions were then applied in a complex setting; the concerted labeling of two target proteins – a 5-substituted triazine was attached to nanoluciferase, and a GFP-cyclopropene was generated through genetic code expansion. TMTH and a tetrazine was added to the mixture, all the proteins reacted, and zero cross labeling was observed.[21]

Computations were used to explore possible IED-DA cycloaddition abilities of triazines, and successfully exposed a scaffold possessing unique reactivity that can be exploited in orthogonal bioorthogonal chemistry.

X The Equilibrium Ratio of Allylic Azide Rearrangement Isomers is Predicted through DFT[23]

Allylic azide, or Winstein, rearrangement

Allylic azides are investigated computationally for the relative populations of isomers at equilibrium: these species interconvert rapidly at room temperature, this process is a 3,3 sigmatropic rearrangement known as the 1,3-allylic azide rearrangement, or the Winstein rearrangement, involving an intramolecular shift of a σ-bond with the ensuing π-bond rearrangement in a concerted process.[23] Prior research has examined the potential utility of specific isomers, where they would be initially isolated via cycloaddition reactions or similar. Determining the ratios of isomers as well as the origins of their respective propensities, as well as the mechanism of their interconversion, is necessary in order to characterize these azides and eventually exploit them for synthetic and other application.[23]

A series of primary, secondary and tertiary azides, along with their (interconversion) transition states and intermediates were optimized at the M06-2X/6-31+G(d) level of theory.[23] IRC calculations verified the transition states and established their connections to products and reactants. Where either side of a C=C is unequally substituted, two energetic pathways are considered, based on two transition states – *endo* and *exo* – for a cis or trans product, respectively, which can further transform through a second transition state to a slightly more energetically demanding conformer, then through a third TS for the *trans/cis* product. These further optimizations were performed at the SMD M06-2X/6-31+G(d) and SMD M06-2X/def2-TZVP levels of theory, in chloroform. The latter is a larger basis set, to assess whether the populations would be more accurately portrayed. Vibrational frequencies confirmed minima and TSs, following which, single point energies were calculated at M06-2X/cc-pVTZ, denoted $\Delta E_{e,o}$, where (for each conformation) Gibbs free energy or $\Delta E_e = \Delta E_{e,o} + \Delta G_s$ (the relative solution free energy calculated at SMD M06-2X/6-31G(d)). Gibbs free energy was compared to previously observed experimental populations – estimated from NMR – and were relatively consistent.[23]

Free energy profiles with *endo/exo* pathways were constructed for each azide with its regioisomers, TSs and intermediates. Low activation energies for the TSs of < 30 kcal/mol confirmed readily occurring rearrangements. Forming bond lengths of TSs showed a concerted, synchronous mechanism (asynchronicity of 0.009-0.037 A° for the *exo* processes, and similarly low discrepancy for the *endo*). Weak hydrogen bonding between OH and azide groups provided some stability for TSs with resulting enhanced population. The populations are controlled by the stability of the C=C bond, dependent on its substituents – greater substitution results in increased stability. The interconversion between 1°, 2° and 3° azides was also investigated; 2° and 3° rearrange faster than 1° azides so 1° azides are more populous at equilibrium, this again ties into the thermodynamically favored C=C with the most substituents. This remains in effect even when H-bond stabilization is a factor.[23]

CuAAC was employed to intercept 1° azides which were exclusively converted to the triazole cycloaddition product in the presence of 3° azides (utilizing an azide from the study which interconverts between a 1° and 3°). A mix of 2° and 3° azides resulted in the trapping of the 2°; whereas a 1° and 2° azide mix did not result in selective interception. As well, these results indicate that the interconversion occurs faster than the cycloaddition.[23]

This theoretical investigation unveiled a concerted, synchronous sigmatropic rearrangement occurring readily for allylic azides. DFT produced relative populations and elucidated contributing characteristics. Computations were performed at multiple levels of theory and reproduced experimental results reasonably well, displaying thermodynamically controlled rearrangement – that free energies predict equilibrium ratios – and also explained the selective trapping with cycloaddition reactions. The reliability of DFT in elucidating the pathways in organic reactions is once more demonstrated.

XI Discovering the Mechanism for the Diazonium Salt + Azide Ion Reaction Yielding Aryl Azides Using Radiolabeling[24]

Potential Energy Surface (PES), IRC, Electrostatic Potential Maps along with Carr-Parrinello Molecular Dynamics Decode an Elusive Reaction Mechanism[24]

Synthesis of aryl azide from diazonium salt and azide ion

Organic azides are prevalent in chemical synthesis, particularly in the formation of heterocycles through Huisgen cycloaddition and Staundinger ligation – which involves an amide bond formation, and has been a rapidly evolving field in the past few decades as the application of the Staudinger reaction in bioconjugation and protein and peptide synthesis and the labeling of biomolecules, where amides are ubiquitous.[25]

Aryl azides are known for their high stability, one method of preparation of aryl azides is through reacting diazonium salts with azide ions, however its mechanism remains elusive.[24] Three possibilities include: 1. S_N2 Ar; or 2. a [3+2] cycloaddition followed by a retro-[3+2] reaction; or 3. an addition/elimination via an

acyclic intermediate. Evidence thus far may indicate the third option is likely, but the nature of it – stepwise or concerted, etc. – requires clarity as well.[24]

By radiolabeling reactants according to the following two schemes, experimental evidence can be gleaned that narrows down the mechanism options. In the first scheme, a non-radiolabeled diazonium salt is reacted with a ^{13}N-labeled azide ion; in the second, the diazonium salt is ^{13}N radiolabeled, the azide ion is not labeled. Each reaction is expected to produce the phenyl azide. Radioactivity was measured for the reaction mixtures, before and after the removal of (radioactive) $[^{13}N]N_2$, the difference is indicative of the amount of radiolabeled N_2 by-product generated, in the first reaction with the labeled azide ion, the N_2 released was almost ~100% labeled, while in the reaction with the labeled diazonium salt, labeled N_2 yield was ~4%. The amount of phenyl azide yielded was double for the latter, indicating a full quantitative transfer of 13N to the product.[24]

Given these results the S_N2 mechanism is ruled out: a labeled diazonium salt reaction would have entirely lost its labeled nitrogen to $[^{13}N]\ N_2$. On the other hand, the cycloaddition mechanism would have generated similar yields of the radiolabeled phenyl azide product via both routes, it is thereby excluded as a possibility.[24]

DFT was then performed on the reaction to gain insight into the now-likely addition/elimination via an acyclic intermediate. Gibbs free energy calculations at M06-2X (PCM)/def2-TZVPP in aqueous solution showed a local minimum on the PES – potential energy surface – of a charge transfer complex (0.5au) with close contact (bond lengths of ~2.4 A°).[24]

The PES is a mathematical depiction of the energy of a molecule as a function of its atoms' positions. Within a molecule, atoms' bonds have varying degrees of freedom (bond stretching), and the energy is calculated as a function of the bond lengths, when each energy of each atom's geometry is incorporated, an energy 'surface' is constructed and it's a highly useful tool in analyzing structure and reaction dynamics, for example stationary points have direct practical significance.[26] Each degree of freedom is essentially a coordinate so dependent on the number in a given system, the PES can be a curve or a surface, they are often computed through a 'scan' where a series of single point energy calculations are performed on an optimized structure or system.[26]

It is interesting to note that this configuration suggested a (concerted) cycloaddition, however the IRC did not connect this TS to a pentazole intermediate; rather it led to another intermediate that indeed forms the pentazole and is followed by the retro [3+2] for the phenyl azide, but this is via a higher energy pathway. IRC scans were performed from the *cis* and *trans* first TSs and led to zwitterionic (a molecule carrying two opposing charges) intermediates for each, while the higher energy *cis* intermediate led to the lower energy second TS to yield the phenyl azide.[24]

The minimum-energy azide anion and diazonium cation interaction complex (that led to the first transition state) was depicted with an electrostatic potential map for charge transfer, and Kohn–Sham analysis for frontier molecular orbital interaction between the salt and anion, with local Fukui indices or f^+ descriptors on nitrogen atoms for electrophilicity (Fukui descriptors indicate areas on a molecule most able to accept or donate electrons). These findings on the proposed complex all align with the third pathway option.[24]

To further confirm, Carr-Parrinello Molecular Dynamics or CPMD – which simulates molecular dynamics using DFT calculations – was performed at different temperatures and found the same complex

(interatomic distances) and zwitterionic structures, stable at 100K and at 300K reached the predicted TS and yielded the phenyl azide product – confirming the stepwise, via acyclic intermediate, reaction that is in agreement with the (radiolabeling) experimental results.[24]

XII The Design of an Azide-Migration Type Synthesis for Regioselective α-Azido Ketones[27]

The Reaction Mechanism and Pathway is Explored with DFT[27]

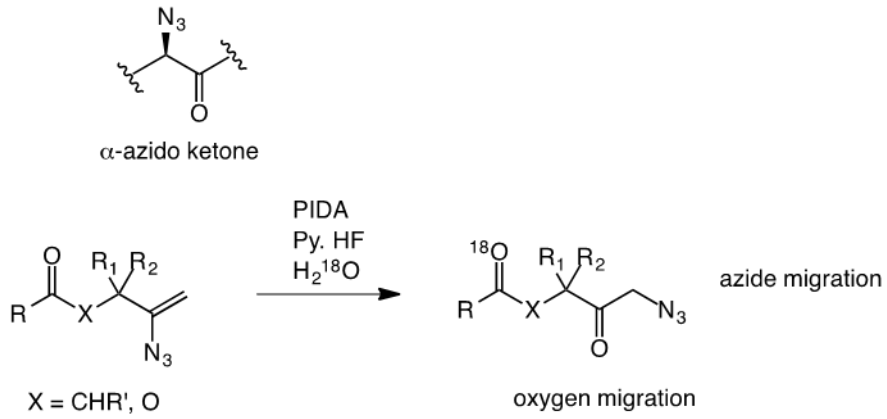

α-Azido ketone; oxygen-migration and azide migration in the synthesis of α-azido ketone from an α-vinyl azide

Organic azides are extremely valuable in both organic synthesis and medicinal chemistry, examples of the former include click chemistry, conversions to amines or nitrenes, Staudinger ligation. Medicinal applications include the introduction of azides into biomolecules and their use in drug discovery. Challenges arise in their synthesis; the simplest approach would be azide migration from a precursor, but migration processes are fraught with fragmentation. The subject reaction is a result of efforts to avoid this molecular breakdown, as well as avoid isomer mixes. The neighboring C=O group assisted azide migration reaction for diverse azido ketones has a fluorine atom driving the rearrangement, and the α-vinyl azide precursor is easily acquired, the azido ketones represent an important class of functionalized azides with much utility.[27]

Experimental work first involved 1,2-azide migrations of 4-azidyl ketones and 4-azido homoallyl whereby optimal reaction conditions, including the $PhIF_2$.HF catalyst, were established. Reactions were then expanded with carboxylate and other EWGs/EDGs around the aryl ring for increased yields. When these enhanced functionalities were added to natural products with vinyl-azide functional groups, the 1,2-azide migration was successfully achieved in some. Further experimentation revealed that α-azido ketones could be yielded from propargyl alcohols (alcohols containing an alkyne functional group) by a tandem azidation/acylation/1,2-fluroiodination/1,2-azide migration, producing in high yield their corresponding α-azido ketone. The mechanism and reaction pathway were explored. Radiolabeling the oxygen atom – ^{18}O provided evidence for 1,4-oxygen transposition along the 1,2-azide migration pathway, likely assisting it.[27]

Theoretical studies provided insight into the regioselective process. An energy profile was constructed with DFT at the M06-2X/6-31G(d,p)/LANL2ZD and included $PhIF_2$.HF and H_2O molecules complexed. Geometry optimizations and frequencies were calculated at B3LYP/LANL2ZD for I and 6-31G(d,p) for the other atoms, with SMD for DCM solvent effect. Vibrational analysis confirmed minima and TS structures, IRC confirmed that the products and reactants connected through the TSs. Single point energy calculations were

performed on computed structures at SMD M06-2X/6-311++G(d,p)+SDD(I) for increased accuracy. NPA – natural population analysis – for atomic charges was computed.[27]

The 1,2 azide shift – facilitated through the complex with $PhIF_2$.HF – was determined to occur via one of two possible pathways with an energy barrier for TS1 and TS2 of 16.0 and 15.1 kcal/mol, respectively, and an overall ΔG of -24.8 kcal/mol. Given experimental evidence that H_2O plays a role, the effects of zero to three H_2O molecules were considered, DFT studies revealed that the TS complexed with two molecules of H_2O was energetically favored in the ring opening step. Similar calculations were performed for the HF elimination step, again favored with two H_2O complexed.[27]

Overall, DFT revealed a 1,2 fluoroiodination, 1,2-azide migration and 1,4 oxygen migration progression, namely an azide shift, nucleophilic attack, ring opening and 1,3-H shift, and finally, elimination of HF. This process is energetically favored, with simple mechanics and short reaction times (>1 min) producing α-azido ketones in high yield.[27]

4. AZO DYES

I Heterocyclic Azo Dyes with Nitrothiazole Groups are Synthesized and Display Exceptional Color[28]

Analysis includes TD-DFT – Time-Dependent DFT – for Electronic Absorption Spectra and DFT for Vibrational Spectra[28]

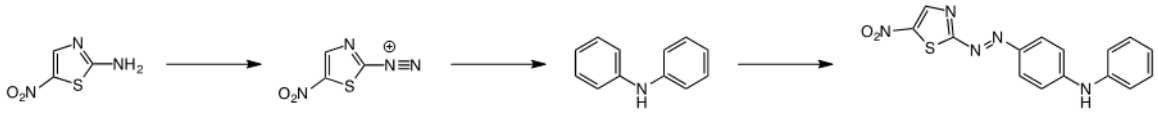

Preparation of azo dye with a nitrothiazole group, through diazotization and reaction with a coupling component

Heterocyclic azo dyes have been favored over their simple aromatic counterparts for superior color, brightness, and fastness. From a biological perspective, these environmentally friendly compounds containing azo moieties have been known to display scavenging and antibacterial activities, also, the thiazole group (which also contributes to the azo dyes' chemistry) is common in biomolecules.[28]

Various 3-amino-5-nitrothiazole-derived azo dyes were prepared through diazotization – a process that converts aromatic amines into their diazonium salts which can then form azo dyes through coupling reactions – forming solid red/orange, red/yellow, dark pink and brown dyes and were studied for their spectral and biological properties.[28]

Antibacterial analysis was done and moderate-to-excellent inhibition was exhibited across the four compounds, with a dye with OH groups performing best. Scavenging properties were investigated by testing different concentrations of azo dyes with DPPH, where the DPPH radical interacts with the H of the dyes and the % scavenging of DPPH is calculated from absorption differences before and after reactions. These scavenging properties are important because non-toxic synthetic antioxidants are sought after, having been found to be more active than those naturally occurring. Again, the same dye performed best due to its OH groups.[28]

Structure optimization and energetic calculations were performed at DFT B3LYP/6-31++G(d,p). Vibrational frequencies and HOMO/LUMO energies were also calculated. TD(time dependent)-DFT is a theoretical method that best calculates the time-evolving energetic parameters of excited systems; including absorption wavelengths the energy associated with $\pi - \pi^*$ transitions of excited electrons and the predicts the spectra and optical properties of organic compounds. It was employed here for electronic absorption spectra calculations, which were compared to experimental absorption spectra in the 200-800nm range performed on the dyes. In both, all the dyes showed two characteristic bands in the UV-VIS spectrum, the first at 261-339nm (318-340nm theoretically) and represents the $\pi - \pi^*$ excited state, from the π electrons of the azo group and aromatic system. The second band is at 566-621nm (418-613nm theoretically) and represents the $n - \pi^*$ transition involving the non-bonding electron pair of N interacting with H from the solvent. Enhanced bathochromic, or redshift was observed, a noted characteristic of the 5-membered heterocyclic azo dyes, this longer wavelength a result of electron-withdrawing properties of substituents. Molar absorptivity was in the 3.8-4.7 range indicating exceptional color for all the dyes.[28]

Computational IR (computed at DFT B3LYP/6-311++G(d,p)) and experimental FT-IR were performed to examine the structure and interactions between atoms/bonds within the molecules as depicted through vibrational analysis, bond stretching frequencies were compared using a linear regression. Additionally, FMO analysis was performed for HOMO/LUMO energy gaps and energy indices because these are valuable parameters for further research.[28]

Diazo dyes were synthesized, experimental and computational research showing them to contain exceptional color, and the unique bathochromic shift and absorption attributed to the five-membered-heterocyclic dyes. There was good correlation throughout between experimental and theoretical results. These dyes displayed antibacterial and scavenging abilities which lend them to biological application, the calculated energetic parameters will aid in expanded research.[28]

II A Disperse Azo Dye with a Pyrazole Skeleton is Investigated Experimentally[29]

A Complete DFT/TD-DFT Characterization with Tautomer, Conformational, Vibrational and UV-VIS Spectral Analysis and NMR[29]

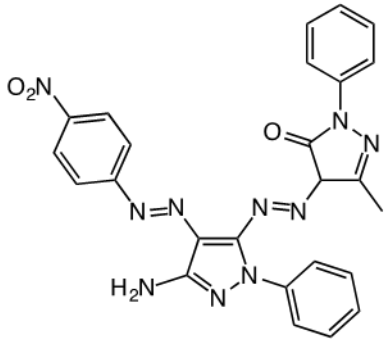

Disperse azo dye with pyrazole skeleton

A disperse azo dye – 4-(4'-(4''-nitrophenyl) azo-3'-amino-1'-phenylpyrazole-5-ylazo)-3-methyl-1-pheylpyrazole-5-one – is synthesized, it is a red crystal. These 4-arylazo-pyrazol-5-one dyes are used in

foods, textiles, and to detect metal ions in spectrophotometry, while the pyrazole moieties are important pharmacologically, including possible anti-HIV effects.[29]

A computational investigation is performed to elucidate its structure. Ground state geometry was optimized at B3LYP/6-311G(d,p). Tautomers were optimized to global minima and the most stable tautomer was determined. Vibrational analysis was performed on the optimized structures, as well as HOMO/LUMO analysis and electronic absorption spectra with TD-DFT at both B3LYP/6-311G(d,p) and CAM-B3LYP/6-31G(d,p). NMR spectra, ^{1}H and ^{13}C, were calculated at B3LYP/6-311G(d,p) with IEFPCM for solvent effect.[29]

Conformational analysis was performed on the most stable tautomer with the potential energy surface scan. The conformational analysis was performed for the three dihedral angles, with the most stable conformation for each compared to the optimized structure measurements for those angles, with the results consolidated for the most optimal structure.[29]

FTIR was performed both experimentally and computationally for vibrational energies. Computational NMR – which has been shown to be valuable especially in elucidating large organic molecules – was performed on the optimized ground state structure with B3LYP/6-311G(d,p) using GIAO (gauge invariant atomic orbitals) and correlated well with experimental NMR.[29]

TD-DFT – known for its precision in these matters – was performed for the UV-VIS spectra, calculating absorption wavelengths and excitation energy. There are two peaks in absorption spectra of the dye indicating that compound is present in multiple tautomeric forms. Since absorption tends to depend on polarity of the solvent, TD-DFT was performed for a series of solvents and calculated excitation energies, oscillator strength, and absorbance at two levels of theory, the CAM-B3LYP results were closer to the experimental.[29]

The calculated absorption spectra λmax represents the HOMO/LUMO transition, and so orbitals and gaps were calculated, specifically the $\pi - \pi^*$ transition between HOMO/LUMO and HOMO-1/LUMO. Since a molecule's excited state is often more polar than its ground state, it will be better stabilized in a polar solvent and will therefore display bathochromic shifts. Similarly, in acidic and basic solvents, hypso- and batho- chromic shifts, respectively, were evident.[29]

The close alignment between experimental and computational results for NMR, FTIR and electronic absorption spectra performed in this research shows the value of this approach and the accuracy of DFT with the stated functionals as a tool in predicting structure and properties of these molecules.[29]

5. BIOLOGICALLY RELEVANT AND BIOLOGICALLY ACTIVE COMPOUNDS

I A Crystallographic and Electron Analysis of a Zn(II)-Azide Complex with a N,N,S-Tridentate Thiosemicarbazone Ligand[30]

DFT Confirmed Structural Parameters and Explained the Intermolecular Interactions Stabilizing the Crystal Structure[30]

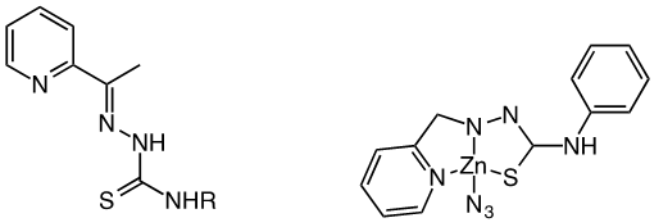

Thiosemicarbazone and zinc(II)azide thiosemicarbazone

A newly synthesized Schiff base metal-azide complex – zinc azide and tridentate chelating ligand thiosemicarbazone – has been found to display excellent scavenging ability.[30] This, and the biological activity being researched and reported as of late for the two individual moieties, compels its complete characterization.[30] Semicarbazones are currently used in the treatment of Chagas disease (trypanosomiasis) and are being investigated as an anti-convulsant.[31] Thiosemicarbazones specifically show wide gram-positive antibacterial capability, as well as antifungal.[31] Their metal complexes have been found to exhibit anti-tumor and anti-neoplastic qualities, effective against solid tumors as well as anti-leukemia and lymphoma activity. They are being studied for anti-viral and anti-amoeba potential and as a radiopharmaceutical tracer/radiotherapy agent.[31] Zinc azide complexes have displayed anti-breast cancer activity as well as antibacterial effects. As metal complexes are increasingly being designed, the study of their structural and electronic properties becomes important.[30]

Experimental analysis includes FTIR, elemental characterization and single crystal X-ray diffraction. Computationally, crystallographic coordinates are used as a starting point for optimization. DFT calculations were performed at PBE0 – a hybrid functional that combines the HF approximation and the Perdew, Burke, and Ernzerhof approximation for the exchange and correlation energy of electrons – with the def2-TZVP basis set for Zn and 6-311++G(d,p) for the other atoms. The found stationary point on the PES was then fully optimized followed by vibrational frequency analysis to confirm it as a true energy minimum. Mayer bond order analysis was performed for bond order indices of the coordination sphere, NPA for atomic charge distribution, NBO analysis and QTAIM – Quantum Theory of Atoms in Molecules – for electron density analysis.[30]

Stretching bonds – from the vibrational frequency analysis – are in strong agreement with literature values. It is interesting to note that among complexes of the same ligands with differing metallic centers, there are differences in C – N and C – S bonds that indicate the influence of the metal-ligand interactions.[30] The ORTEP diagram from X-ray diffraction shows the Zn four-coordinated with the tridentate chelating thiosemicarbazone ligand (which donates three bonds to the Zn, from two Ns and S) and the azide anion. The DFT and X-ray crystallography geometries were very closely aligned, despite DFT being performed on a single crystal and crystal packing affecting experimental results. The slight differences included azide

group and aromatic rings orientations. Bond lengths and angles were compared across the X-ray, PBE0 and BO index (characterizes bonds as σ, π or triple). Almost all results were closely aligned, but within the azide group, the two N – N bond lengths are similar however BO analysis has one as σ, the other π.[30]

A look at the optimized structures of triplet and quintet energy states gave a very large energy gap, depicting the complex's low spin state. Electric dipole moments were calculated.[30]

FMO analysis revealed the N and S lone pairs, and to an extent the Zn's d orbital, as the main contributors to HOMO, the pyridine and coordination sphere's C – N bond, to the LUMO. The energy gap of 3.5eV was within common range for Zn complexes. MEP defines the reactivity of a molecule based on charge distribution, which is significant when considering the molecule employed in a biological system and potentially engaging in nucleophilic/electrophilic reactions. Electrophilic regions were shown near Zn and ring-Hs, nucleophilic around azides and aromatic centers.[30]

Hirschfield surface analysis based on crystallographic data predicts intermolecular stabilization by looking at electronic densities of different areas that represent interatomic contact. It showed NH ---N hydrogen bonds and C – H ---π bonds as most responsible.[30]

DFT was employed to further elucidate the dimer structure and interaction and calculated a modest interaction energy mostly due to azide-amine H-bonding, the optimized and experimental bond distances of which were in good agreement. Second order perturbation theory analysis with NBO shows a charge transfer from the lone pair into this bond of 9.1 kcal/mol. For further insight into the nature of these intermolecular interactions, QTAIM showed bond critical points for NH---N, S---S and CH---N (azide and rings), with a series of parameters – namely the electronic charge density [$\rho(r)$] with its Laplacian [$\nabla^2 \rho(r)$], the total energy density [H(r)], relationship between local potential energy and the gradient kinetic energy [$|V(r)|/G(r)$], and ellipticity (ε), – further and more definitively characterizing these H-bonding interactions as having ionic character.[30]

Overall, this study found computations to be in very close alignment with experimental results, characterizing a Zn center coordinated by a tridentate thiosemicarbazone ligand and an azide anion, the crystal packing details consisting of a dimer arrangement in the unit cell, for which DFT was productively employed to elucidate the stabilizing forces.[30]

II Mono- *and* Bis-*Alkylated Lumazines are Synthesized as Potential Membrane-Bound Photosensitizers*[51]
Theoretical Studies with Molecular Orbital Theory and Mayr's Nucleophilic Index Provide Insight into Alkylation Patterns[51]

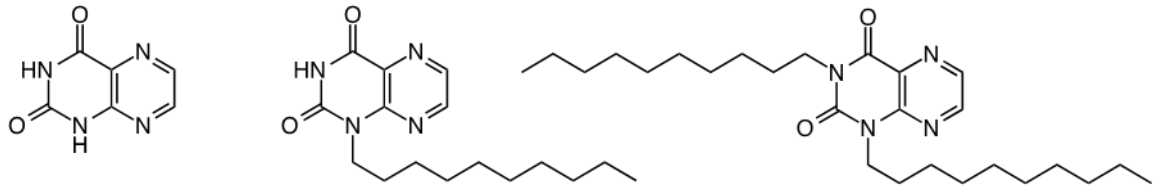

Lumazine; mono-*alkylated lumazine;* bis-*alkylated lumazine*

Lumazines are pteridine derivatives. Pteridine were first discovered as pigments that are found in many insect wings and eyes, and in small amphibians. Pteridine compounds are composed of a fused pyrimidine

and pyrazine ring. Pteridines of multiple forms are widespread in biological systems, playing various roles. Oxidized pteridines are able to fluoresce, undergo photooxidation and produce reactive oxygen species. They are efficient photosensitizers and can photo-induce cell death and oxidation of biomolecules. Two compounds belonging to this family are pterins and lumazines, they are both fully oxidized aromatic pteridine derivatives.

Previous research on decyl chain conjugation to pteridine compounds, seeking to increase their solubility in organic solvents and increase their affinity for the phospholipid membranes, has been successful. A pterin had been synthesized with the anticipated properties as a membrane intercalator, a fluorophore and a singlet molecular oxygen sensitizer. These properties allowing it to be a self-monitoring membrane fluorescent probe and a membrane photo-damaging agent. The current study is focused on decyl chain conjugation of its relative, lumazine, alkylated in an S_N2 reaction, also looking for increased solubility in organic solvents and seeing what photophysical properties arise. The reaction products – one *mono* alkylation product and one *bis* alkylation product – were characterized with NMR. Computational studies were performed to understand their patterns of alkylation, which occurred at N sites of the pyrimidine ring, at the exclusion of O sites, producing only one of two possible N *mono*-alkylated products (N1). B3LYPD95(d,p) level computations for optimized structures of the proposed *mono* and *bis* alkylated products at N and O sites. Molecular orbital calculations for HOMO and LUMO and Mayr's nucleophilicity parameter *N* was used to analyze the alkylation reaction. DFT structural optimizations and energetics were carried out for computed Gibbs free energies and ΔG explained alkylation at N vs O sites, the former being significantly favored energetically. Still unexplained is the absence of the second *mono*-alkylated product (N3). HOMO and LUMO studies, corroborated by Mayr's nucleophilicity analyses, showed a lack of *p*-orbital at N3 making the alkylation improbable, but following the alkylation at N1, a *p*-orbital emerged at N3 allowing for the second iododecane equivalent to react with the lumazine.

The experimental components of the research found that the alkylation increases the compounds' lipophilicity for greater plasma membrane binding capabilities, and photochemical properties studied included increased fluorescent quantum yields and similar emission spectra relative to the parent compound, all of which compels further research into possible biochemical application as a membrane bound photosensitizer.

III The Debated Mechanism of Hydrolysis of Hydrazones is Clarified Through DFT Thermodynamic Calculations and a pH–Based Stability Inversion of Triazinyl Hydrazones is Examined[32]

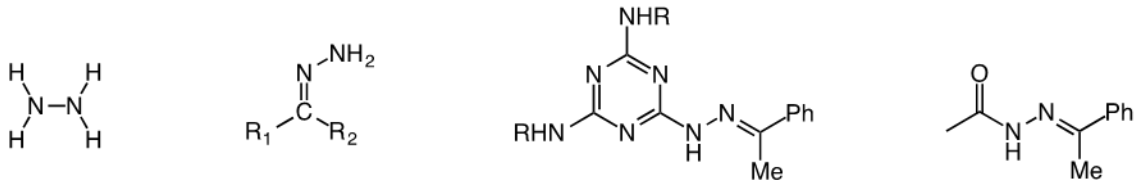

Hydrazine; hydrazone, synthesized via reaction with aldehydes and ketones; triazinyl hydrazone; acyl hydrazone

Hydrazones and hydrazone chemistry are widely used in organic synthesis and molecular biology, including as an anti-trypanosomal and as a linker in drug conjugates, the latter a product of its acid-lability. Many

hydrazine derivatives (including aromatic, acyl and aliphatic) have been studied, but the mechanism of hydrolysis of the hydrazones has not been uncovered.[32] Herein, the possibility of triazinyl hydrazines as a comparable species to the well-known acyl hydrazine is examined for its hydrazone hydrolysis. A series of five aldehydes and ketones and hydrazine were condensed to form the hydrazone product; as well as the corresponding acyl hydrazones. All ten hydrazones were then hydrolyzed at specific pH levels – 5.2, 6.8 and 8.0 and monitored for first order reaction rates and half-life. DFT was performed at B3LYP 6-31+G(d,p) for Gibbs free energy calculations and optimized geometries of all compounds.[32]

It is generally held that hydrazone hydrolysis is initiated with the protonation of the center nitrogen (double bonded to C and single bonded to the second N), followed by the addition of H_2O yielding a carbinolamine, followed by proton migration to the central nitrogen and the cleaving of the C – N bond.[32] The main influence on reaction rate – rate varies significantly with different hydrazones – is the subject of contention, alternately proposed to be a result of thermodynamics; resonance stabilization that affects C adjacent to N; or protonation resistance of the central N.[32]

DFT calculations are employed for ΔE of protonation. Experimental results show pronounced hydrolysis at a pH of 5.2, with the acyl counterparts displaying more stability (lower reaction rates) as compared to the corresponding triazinyl hydrazones.[32] Within the two groups, the same trends are followed for relative stabilities of derivatives. At pH of 6.8 hydrolysis was fractional, at pH of 8.0 it was negligible. The experimental rates of hydrolysis were in direct qualitative correlation with DFT computed proton affinities, where greater half-lives were associated with small or negative proton affinity. Proton affinity was greater for the triazinyl than the acetyl counterpart for each derivative, along with a greater reaction rate. This is in clear support of the hypothesis that proton-affinity is the main driver of the reaction rate.[32]

Necessitating further consideration is the fact of the triazine moieties' own protonation sites. Whereas the pKa of the central N is extremely low, the pKa of triazines is at approximately 5, and so hydrolysis must be considered at a lower pH where a protonated triazine might result in increased central N resistance. Indeed, computations depicted a decreased proton affinity by 4.1 – 5.0 kcal/mol with a protonated triazine group (more so with ortho protonation). To quantify the effects, hydrolysis was performed at pH of 4.0 and indeed, an inversion of relative stabilities was immediately evident, with reaction rates and half-lives of the triazinyl hydrazines now significantly lower than the acetyl counterparts.[32]

A combined computational and experimental approach was successful in supporting a 'resistance to protonation' hypothesis regarding the mechanism of hydrolysis of hydrazones. The inversion of stability of triazinyl (vs acyl) hydrazones at a lower pH is a property potentially exploited biologically.[32]

IV A Newly Identified Reciprocity Between Two Important Phenomena – Hydrogen Bonding and Aromaticity in Hetereocycles[33]

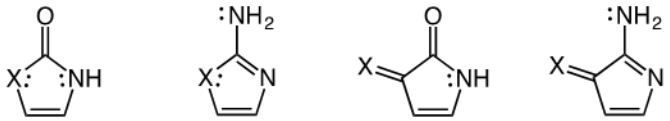

An amide with a 6πe⁻ system; an amidine with a 6πe⁻ system; an amide with a 4πe⁻ system; an amidine with a 4πe⁻ system

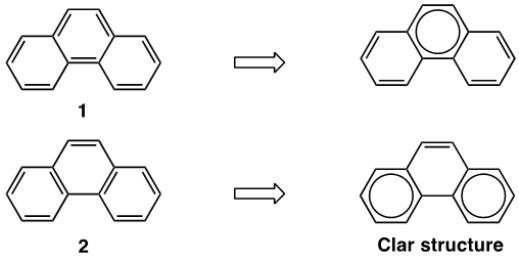

A Clar's sextet structure: compound 2 is considered the significant resonance form giving two aromatic systems

AMHB – antiaromaticity or aromaticity modulated hydrogen bonding – is a relatively recently observed effect; the reciprocal nature of hydrogen bonding and aromaticity.[33] Hydrogen bonds polarize π conjugated systems and thereby perturb the delocalized electrons, either enhancing or diminishing their aromatic or antiaromatic character.[33] Dimerized (or otherwise complexed) heterocycles with the same kind of H-bond donors and acceptors will have differing association energies, based on their conjugated πe- systems. The polarization induced by the H-bonding can either enhance or disrupt an aromatic system (conjugated, $4n+2$); intensify or relieve and antiaromatic system (conjugated, $4n$).[33] Modeling dimers of aromatic, nonaromatic and antiaromatic monomer analogs, the modulation of the H-bonding is described in terms of the interaction enthalpy – $\Delta_{dimer}H$ – for two different cases. In the first, the aromaticity is enhanced and antiaromaticity intensified in the respective monomeric units upon dimerization, enhanced aromaticity is concurrent with a larger $\Delta_{dim}H$ than the non-conjugated analog, and intensified antiaromaticity reflects the smallest $\Delta_{dim}H$. in the second case, H bonding that disrupts an aromatic system has the smallest $\Delta_{dim}H$, and where the antiaromaticity is relieved, the largest $\Delta_{dim}H$. Changes in bond lengths show the electron polarization affects that promote the particular resonance form – electrons move from the double bond towards the atom that is the H-bond acceptor. The new single-character bond is lengthened, the double bond is reflected by a shorter bond length.[33]

Individual aspects of AMHB have been addressed in research, but here a broader pattern is sought out, through quantum calculations, to describe the relationship of H-bonding and aromaticity. This is achieved by looking at a series of five-membered heterocycles, many of which are the framework, or representative of a part thereof, of biomolecules or pharmacological privileged scaffolds and as such, this concept is potentially significant in these fields.[33]

Monomers and dimers were fully optimized at PBE0/6-311++G(3df,3pd), which when benchmarked against the highly accurate CCSD(T) had a very low mean absolute error. Frequency calculations were performed to confirm stationary points. Dimerization energies were computed as $\Delta_{dim}E = E_{dimer} - 2E_{monomer}$ and the $\Delta\Delta E_{dimer}$ is the difference in dimerization energies of the conjugated systems and their non-conjugated reference molecules.[33]

Nucleus independent chemical shifts – NCIS – with (1)zz – removes σ contributions – is computed at 1 A° above ring centers to quantify changes in aromatic/antiaromaticity upon dimerization, a negative value indicates increased aromaticity (diatropic character) or decreased antiaromaticity (paratropic character) (depending on the type of molecule).[33] NCIS(1)zz analysis was performed on the monomers, then on the individual rings of the dimer, and displayed the H-bond induced antiaromatic or aromatic effects, for each of the four scenarios mentioned above.[33]

In the first case, where H-bonding (favored resonance form) enhances aromaticity, NCIS values for the selected heterocycles became more negative in dimer form: an original range of -14.9 – -12.0ppm went to -16.7 – -13.5ppm. This corresponded with aromatic heterocycle to non-conjugated analog $\Delta\Delta E_{dim}$ range of -2.9 to -4.4, reflecting strong H-bonding interaction. In derivatives of these heterocycles where adjacent atoms' lone pairs form part of the delocalized electron system, an even more enhanced aromaticity is observed ($\Delta NCIS(1)_{zz}$) and attributed to the easing of this lone pair repulsion, where the N – X (the involved atom pair's bond) is shortened with increased H-bond interaction. [These observations were made using experimentally determined H-bond acceptor/donor distances from the Cambridge Structural Database. A series of derivatives, enhanced-type vs disrupted-type aromatics were averaged and the effect on bond length of the aromatics vs non-aromatics for the enhanced vs disrupted aromaticity were compared].[33]

In the three other cases too, these patterns persist: H-bond weakening upon disruption of aromaticity, $\Delta NCIS(1)_{zz}$ are less negative showing decreased aromatic character upon dimerization, ΔE_{dim} are smaller than their non aromatic analogs (positive $\Delta\Delta E_{dim}$).[33] Lone pair repulsion is increased, lengthening the N – X bond and therefore further weakening the H-bonding interaction. When investigating antiaromatics, again, where H-bonding intensifies antiaromaticity – enhanced cyclic 4πe- delocalization – it is weakened, and where it relieves antiaromaticity, it is strengthened. The increase in antiaromaticity is shown with positive shifts in NCIS values.[33] Where delocalized N lone pairs are neighbored on either side with electron withdrawing groups (EWGs), the pair is 'isolated' and there is a smaller enhancement of antiaromaticity, and less weakening of the H-bond interactions relative to the nonaromatic system. H-bonds are strengthened by the disruption of antiaromaticity; NCIS shift in the negative direction, i.e., smaller positive values show a decreased antiaromatic delocalization, with more favorable dimerization energies than the non-conjugated analog.[33]

The pattern of reciprocity between hydrogen bonding and aromaticity having been consistently demonstrated, a two fused imidazole ring – 1H-imidazo[1,2-a]imidazole – was presented as a framework for tuning dimerization energy by hydrogenating different double bonds,[33] forming a Clar's sextet – where in multi-ring systems, π aromatic systems are classified as 6π electrons localized in a ring separated from the adjacent rings by a C – C single bond, and the resonance structure that has the most separated aromatic sextets is the most important in characterizing the system's aromatic properties.[34] This particular framework has H-bonding enhanced in the resonance form that bears a Clar's sextet (with the other sextet disrupted), and $\Delta NCIS(1)_{zz}$ values for both rings show decreased aromaticity for the aromatic ring and enhanced aromatic character for the non-sextet.[33] Compared to the nonaromatic 2 ring system, there is more favorable dimerization energy and, as published crystal structures show, shorter H-bonds for the conjugated system. In an analog where the Clar's sextet aromaticity is enhanced, and there is no sextet (disruption) in the other ring, even more favorable dimerization interaction energies are noted. In another analog, dimerization disrupts aromaticity ($\Delta NCIS(1)_{zz}$ values reflect this) in the sextet, weakens H-bonding and the dimerization energies are less favorable than the non-conjugated system.[33]

This framework investigation strongly suggests the tunability of hydrogen bonds in aromatic systems.[33]

This exploration of 24 selected heterocycles has provided an encompassing picture of how hydrogen bonding and aromaticity or antiaromaticity effects interplay. This was achieved using computations of energetics – ΔE_{dim} and $NCIS(1)_{zz}$. This deeper insight into these parameters are important in understanding the chemistry of heterocycles that are so ubiquitous in biological systems.

V Aromaticity-Modulated Hydrogen Bonding in Biologically Important Heterocycles[35]

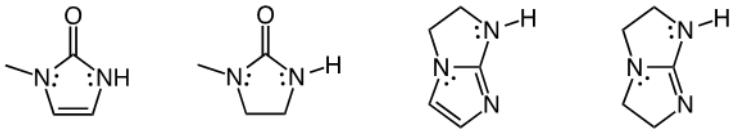

An aromatic heterocycle present in thymidylate kinase inhibitor; its antiaromatic analog; a structure similar to biotin; its antiaromatic analog

Heterocycles are prevalent in biomolecules, and two major characteristics often found in heterocycles – aromaticity and hydrogen bonding – play essential roles for example in drug-receptor binding, enzyme cofactors and stabilization of the DNA double helix. Building on the recent research on AMHB – which describes a relationship between these two phenomena – two heterocycles were analyzed experimentally and computationally for the aromaticity effects of hydrogen bonding on the molecule. The molecules were chosen based on their heterocyclic framework derivatives being found in biological compounds active in ligand-protein binding through H-bonding; Compound A, a thymidylate kinase inhibitor; and Biotin, a vitamin.[35]This was done by investigating dimers and non-aromatic analogs of the two chosen molecules – one where aromaticity is enhanced by H-bonds and the other where aromatic delocalization is weakened.[35]

Geometry and structure optimizations were performed at ωB97-XD/aug-cc-pVDZ for all monomers and dimers, vibrational analysis confirmed minima and H-bonding dimerization (interaction) energies were calculated. $NICS(1)_{zz}$ was computed at mPW1PW91/6-311++G(3df,3pd)//ωB97-XD/aug-cc-pVDZ for changes in aromatic character. Dipole moments came from MP2/aug-cc-pVTZ single point energy calculations for the monomers, based on their dimer geometries.[35]

Computational $NCIS(1)_{zz}$ correlated well with experimental results and showed increased aromaticity or a negative Δ for the heterocyclic compound in which H-bonding enhances aromaticity, this was accompanied by $\Delta_{dimerization}H$ more negative than for the non-conjugated analog. The exact reverse pattern was found for the second compound where H-bonding disrupts aromaticity. Experimental evidence which included single-crystal structures and NMR confirmed the N-H…..N bond distances reflecting the strength of their dimer interactions, shorter when the interaction is stronger, in the case of enhanced aromaticity.[35]

The study provides again a clear illustration of the AMBH effect, and actually quantifies an effect of up to 30% on the H-bonding interaction energy through modification of aromaticity, which has great implication for drug design as well as the understanding of biological interactions where H-bonds are present.[35]

VI ESPT – Excited State Proton Transfer Discovered to Relieve Excited-State Reversal of Antiaromaticity/Aromaticity[36]

TD DFT Calculations for NCIS(1)$_{zz}$ and Energetics Calculated at S_0, S_1 and T_1 States Demonstrate this Relationship[36]

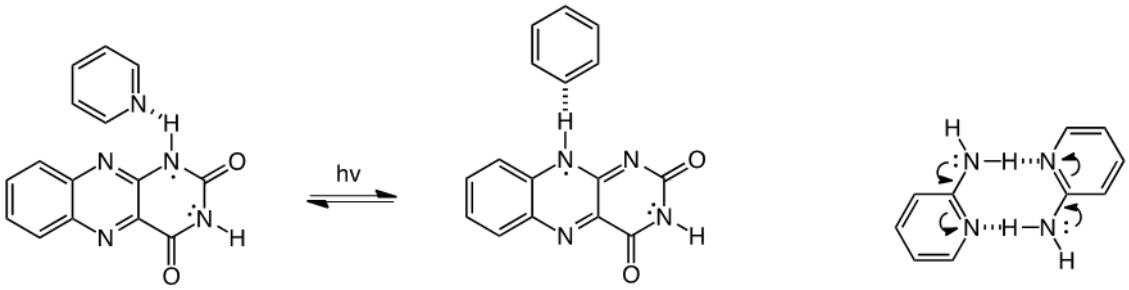

Dynamic catalyzed excited state proton transfer in flavin – flavin-pyridine complex; 2-amino pyridine dimer

Another aromaticity-related phenomenon is excited-state proton transfer or ESPT.[36] When light strikes certain organic compounds, surprisingly elevated rates of intramolecular proton transfer have been observed, understood to be the result of 'enormous' change in the electronic structure of a molecule with varying opinions as to the nature of this change.[36]

Baird originally discovered in the early 1970s that resonance stabilization of conjugated hydrocarbons in the lowest triplet state – $^3\pi\pi^*$ – is the reverse of that in the ground state, where aromaticity and antiaromaticity are based on Hückel's $4n$/$4n$+2 π electron counting rules. In the triplet excited state, conjugated systems or $4n$ π electrons are 'aromatic' and stabilized and those with $4n$+2 π electrons are 'antiaromatic.'[37]

With a computational approach, researchers have herein demonstrated that ESPT is an instrument through which excited-state-induced antiaromaticity is relieved: proposing that Baird's rule regarding the reversal of aromatic and aromatic character in the triplet excited state is the 'enormous change.'[36] Where $4n$ + 2 π conjugated compounds have proton donating and proton accepting groups, ESPT can relieve excited state antiaromaticity. Antiaromatic compounds are difficult to research experimentally due to their inherent instability which further indicates the tremendous value in the computational approach.[36]

There are various types of excited state proton transfers, from a direct intramolecular transfer along a hydrogen bond or by way of a zwitterion intermediate, to dynamic catalyzed transfer – where an independent catalyst/substrate is involved and transfers a H from one position to another within the molecule – for example the biomolecule flavin (three fused heterocycles) – a photoactive cofactor in many enzymatic reactions can undergo proton transfer via a complex with a pyridine ring, that moves a proton from one if its rings to another. Flavins and other compounds examined here are aromatic in the ground state and $4n$ + 2 *anti*aromatic in the first excited state.[36]

Computed NCIS(1)$_{zz}$ values at PW91/IGLOIII//(TD-)ωB97X-D/6-311+G(d,p) – in ppm for the ground – S_0 –, approximated singlet – S_1 – and triplet – T_1 – states for all compounds studied showed a clear reversal of aromaticity between ground and excited states.[36] Tautomerization energy – ΔE_T in kcal/mol (the energy associated with the intramolecular H transfer) – is calculated for each state at (TD-)ωB97X-D/6-311+G(d,p)

where positive values indicate a higher energy form. For each compound at each excited state, aromaticity is measured ($NCIS(1)_{zz}$) for the tautomer with the $4n + 2$ π electron form – denoted A –, and for the breached conjugation system – denoted Q –, and the difference in tautomerization energies is measured. The $NCIS(1)_{zz}$ strongly indicate that the ΔE_T are a direct result of inversed aromaticity/antiaromaticity.[36] At ground state, the $NCIS(1)_{zz}$ values for the A (aromatic) forms are negative and large which shows aromatic character, in the excited states these switch to positive – antiaromatic. The Q forms on the other hand have more positive – more antiaromatic character in the ground state. The direct relationship between the energy states, and reversal of aromaticity is immediately evident. ΔE_T becomes distinctively more negative between the ground and excited states demonstrating the energetically favored proton shift, relief of antiaromaticity.[36]

In this study as well, the reciprocal antiaromaticity/aromaticity-hydrogen bonding effects with dimerization were found.[36]This ESPT and antiaromaticity relationship represent further important discovery regarding aromaticity with tremendous value in understanding the photochemistry occurring in biological systems.

AN IN-DEPTH REVIEW OF SELECTED COMPUTATIONAL INVESTIGATIONS OF IMPORTANT AND COMPLEX BIOLOGICAL AND RELATED COMPOUNDS WITH NITROGEN-CONTAINING HETEROCYCLES

I Adenine, and Purine from which it is Derived are Computationally Explored for Substituent Effect[38]

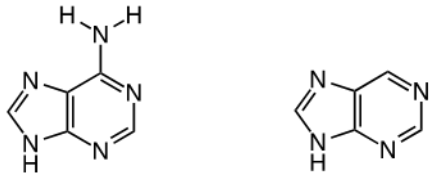

9H adenine and 9H purine, the most stable tautomers of each

Adenine is one of the four nucleobases in DNA and its derivatives feature heavily in biochemical processes including cellular respiration. It is a simple amino derivative of purine and is composed of fused pyridine and imidazole rings.[38] Four endocyclic nitrogens afford it low energy prototrophic properties; it can form four tautomers, one of which, termed 9H has been established as the most stable. Given that these proton transfers occur with a rearrangement of π electrons, it follows that with the introduction of a substituent, the sensitivity of the system to its effect will be a function of the tautomeric form. Much research has been applied to substituent effects on the properties of this important molecule, just a few examples include: their effect on the structure and curvature of both B- and Z- DNA double helix; on polymerase detection of error during base pairing; and interaction energies of A – T pairing. Research implicates substituent effect as a major influencing factor on the properties of the bases, and this study sets out to investigate, using quantum calculations, substituent effect in these complex systems, and how they might vary between tautomers and affect their relative stabilities, as well as the influence of adenine's amino group on these parameters (relative to purine).[38]

Substituent effects have been classically quantified by Hammett substituent constants 'σ' as applied in the Hammett equation $P(X) = \rho\sigma(X) + \text{constant}$ where P is the sensitivity of the system to substituent X and ρ is the reaction constant. Quantum chemistry methods include the quantification of the products' and

substrates' energy difference – SESE – substituent effect stabilization energy based on homodesmotic reactions (those in which the same number of chemical bonds and hybridizations of atoms are maintained); as well as cSAR(X) – charge of the substituent active region – that relates σ to the total charge of X and its ipso carbon atom; and MESP – molecular electrostatic potential analysis.[38]

Research herein looked at adenine and purine derivatives substituted at the C2 (pyridine ring), C8 and N7 (imidazole ring) sites, where a series of ten substituents (X) range from EDGs to EWGs – NH2, OH, OMe, Me, H, F, Cl, CHO, CN, NO2. Calculations were performed with DFT B97D3 with aug-cc-pvdz, optimization of all structures was performed, and said structures were confirmed as minima on the potential energy surface with vibrational frequency calculations. The four most stable tautomers of both adenine and purine are termed, in order of decreasing stability: 9H, 7H, 3H and 1H. First explored was the ΔE between the most electron withdrawing substituent – NO_2 – and the most electron donating substituent – NH_2 – at each of the three substitution sites (C2, C8, N7) for each tautomer of adenine and purine, it was immediately evident that the C substitutions caused a decrease in energy of the system relative to the N position. Also, in the case of the X = NH_2, while demonstrably more stabilizing (as an EDG) across the board, significant impact of the group was noted on the *relative* stabilities of the tautomers. Relative energies were calculated for each of the 1H, 3H and 7H tautomer derivatives relative to the 9H (in all cases, the most stable): for the adenine derivatives, the average $\Delta E_{relative}$ was ~10 kcal/mol, for the purines ~7.3 kcal/mol, this increased variability stems from the NH_2 groups.[38]

To further analyze substituent effect, the ΔE_{rel} values were used in reference to unsubstituted tautomers (X = H), using homodesmotic reactions and denoted $SESE_{rel}$: essentially the relative effect of the substituent on the specific tautomer relative to the most stable tautomer, 9H. This model allowed the conclusion that the most significant substituent effect is in adenine, when the X is on the imidazole ring. Substituent effects were then compared between the C2 and C8 positions for adenine and purine derivatives individually: showing that the nature of the effects differ between the molecules, but they are similar in intensity.[38]

SESE were then investigated for relative effect on adenine vs purine, using homodesmotic reactions, where differences in energies of effects in adenine are a result of its amino group; The $SESE_{PU}$ values indicate a more stable substrate (purine) when positive and were usually positive for the EWGs and negative for the EDGs. These $SESE_{PU}$ values were compared with the Hammett constants described earlier: good correlation exists between the C8 substituted $SESE_{PU}$ and the *para* σ, and the C2 position with the *meta* σ.[38]

Next was a comparison to the classical models in substituent effect research: benzene and aniline, results further point to the amino group reducing substituent effect, more evidently at C8 vs C2.[38] Given the fused imidazole and pyrimidine ring structure of the purine/adenine, the SESE was applied to compare effects in these 'separated' rings. Plotting the descriptors against the adenine and purine values displayed a linear relationship and showed that the amino group of adenine reduces substituent effect.[38]

Given the obvious influence of the amino group of substituent effect patterns, a correlation between the cSAR of NH_2 and the $SESE_{purine}$ for all the adenine tautomers was plotted and analyzed: the determination coefficients displayed a strong correlation, and an increased variability in slopes (of the different tautomers) of the C8-X relative to the C2-X, which is explained in terms of resonance stabilization, where the C8 – substituted position for adenine acts as a para substitution pattern, the resonance forms in turn affected by the differing tautomeric positions.[38]

SESE – substituent effect stabilization energy – was successfully employed with various reference systems as a tool to analyze different aspects of substituent effect. In all cases, the 9H tautomer was the most stable, the 1H the least, and the 7H and 3H varying with influence of the NH_2 group. This group promoting, in general, greater disparity in energy across tautomers. $SESE_{relative}$ showed that where a substituent is adjacent to the given tautomeric position, a stronger substituent effect is evident in adenine. Additionally, substituents at C8 have a greater effect in adenine. The $SESE_{PU}$ demonstrated that these effects are due to stabilizing interactions with EDGs and destabilizing interactions with EWGs, more pronounced at C8. Monocyclic system comparisons allowed for the conclusion that between adenine and purine, the amino group reduces substituent effect. SESE descriptors, well correlating with Hammett constants permitted comparison between the subject compounds and benzene and showed the para and meta positional influences on the systems, and the role of resonance in such. This study highlights the utility of quantum calculations in partnership with traditional chemistry methodologies in exploring reactivity and effects in complex systems.

II Folic Acid Photodecomposition – DFT Investigates the Exact Nature of this Breakdown[39]

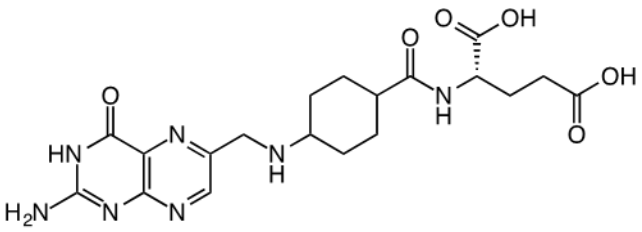

Folic acid

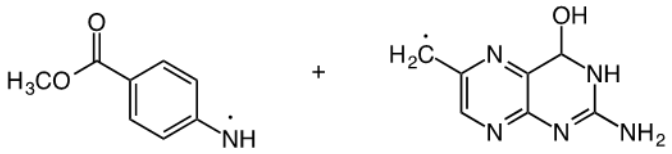

Folic acid photodecomposition radical products of bond cleavage (methyl-ester analog for Glu for computational simplicity)

Folic acid is a very important biomolecule, active in many metabolic processes, and central to this study, photochemical processes such as photosynthesis. Its photochemical abilities are being researched for possible photosensitizing-based cancer treatment.[39] (Photosensitizers are excited to their singlet state, then, through intersystem crossing (ISC) convert to triplet state, which is prolonged with spin flipping, allowing the photosensitizer to interact with surrounding molecules). Here, researchers aim to investigate the mechanism of FA's photodegradation; understand the intramolecular processes that may be involved in its photochemistry; elucidate the role oxygen may have in these processes. Folic acid is composed of pterin, p-amino benzoic acid and glutamic acid, linked in that order.[39] When irradiated, the bond between the pterin ring system and PABA is cleaved. Pterin and its derivatives are reported to have quantum yields in aqueous solution that range from ΦF = 0.07-0.33 at a 350nm excitation; whereas FA has a very low ΦF <0.005. (Fluorescence involves the absorption of a photon of light bringing the species to an excited state, followed by the emission of light at a lower energy (longer wavelength) as the compound relaxes back to

ground state). It is understood that the reduced quantum yield is a result of intramolecular quenching, however the nature of this quenching remains unknown.[39]

Folic acid is structurally somewhat similar to riboflavin, another photosensitive vitamin that has a high fluorescent quantum yield that is drastically reduced when it is in FAD (flavin adenine dinucleotide) – a photostable compound – and this is because of a photo-induced electron transfer followed by a back electron transfer that occurs through space and dissipates the absorbed photon energy.[39] This suggests a similar process may occur in folic acid and that the electron transfer product is a reaction intermediate. DFT studies are herein performed to uncover the intramolecular mechanism of FA's oxygen-independent photodecomposition. Free energy calculations and vibrational analysis for the structures were performed at B3LYP/6-31+G*//B3LYP/6-31G* with PCM with water as a solvent. NPA – natural population analysis – was performed for atomic charges and spin densities.[39] Experimental methods included absorption and emission spectra, manipulation of which enabled estimation of singlet excited state energy, the pterin was selectively excited (PABA can be excited as well) by selecting an appropriate wavelength of light. The singlet excited state of the pterin of FA was estimated at 70 kcal/mol above ground state, which is very close to unsubstituted pterin and allows for it to be used appropriately as a model in the theoretical investigation.[39]

DFT thermodynamic calculations were done on models of the PABA and pterin moieties of FA to look at the photo induced electron transfer. Glu was replaced with a simple methyl ester and the pterin ring system was substituted with a methyl group. 'Dividing' FA into two model compounds isolated the charges to the individual π systems which allowed energy to be calculated on this model charge-separated (radical ion) species that follows the electron transfer, and following bond cleavage, the energy of the radicals above the ground state, can be calculated at 42.2 kcal/mol. NPA analysis of the radicals and radical ions looked at spin density (in radicals, refers to unpaired electrons) and charge. Visualizing the atom(s) with the most spin density, along with the atom(s) with the most negative charge, allows for the likely resonance structure to be determined for the pterin radical, post electron-transfer reaction. Parallel considerations are used for the cationic radical species, and after the ensuing bond cleavage, two neutral radicals are likely produced.[39]

DFT calculations support the proposed mechanism: the pterin is excited to the singlet state following photo absorption, at 70 kcal/mol above ground state; an electron is transferred to the PABA ring and the two moieties are now a charge separated radical ion pair, the energy calculated at 58.1 kcal/mol – the process being exothermic. Pursuant back electron transfer 'through-bond' resulting in bond cleavage is determined to be thermodynamically favored. The resonance structures allow for a complete proposed pathway for the photo-induced electron transfer and photodecomposition of FA.[39]

III An Examination with DFT of the Breakdown of the Folic Acid under Hydrothermal Treatment[40]

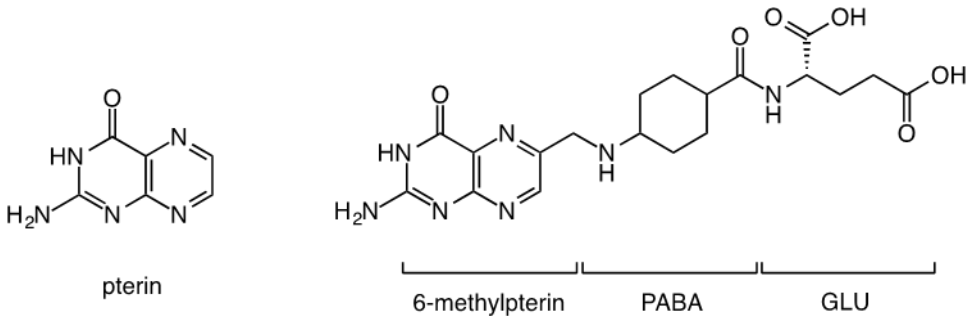

Pterin – parent compound; FA components – MPT is responsible for folate receptor binding and fluorescent emission, PABA plays a role in non-radioactive relaxation via intramolecular charge transfer, glutamic acid

Folate is an essential B group vitamin, and requisite in many biological processes and intracellular reactions including the metabolism of amino acids and DNA and RNA synthesis. It is also a participant in photochemical processes, including photosynthesis. Though its biochemistry is very wide ranging, of significant research focus as of late is its folate receptor binding capabilities: folate receptors, for folate uptake, are present on most cells. However, many tumor tissue cells overexpress folate receptors, particularly the FRα to meet the elevated folate demand of their rapidly dividing cells. This property has been exploited in medicinal chemistry and is the basis for targeted therapies, and imaging, by conjugating the agents to folic acid that will bind to the receptors.[41]

Most recently, researchers have synthesized carbon nanoparticles or 'quantum dots' by heat treating folic acid.[42]Quantum dots are highly advantageous in optical bioimaging, being chemically inert and photostable, with tunable, strong photoluminescence. These unique characteristics provide unprecedented potential opportunities in optical bioimaging, and phototherapy.[43]

Combining these two attributes of exploiting folic acid receptor binding with the photophysical properties of quantum dots (graphene dot) was recently discovered as possibility; the hydrothermal treatment – HT – of folic acid, as the singular precursor was able to produce these carbon nanoparticles – with extremely high quantum yield. Biocompatible by nature and retaining their receptor-binding moieties, these quantum dots have tremendous potential in therapeutic and bioimaging applications.[42]Structurally, FA is composed of a pteridine ring – 6-methylpterin, or MPT; p-aminobenzoic acid, or PABA; and glutamic acid, Glu (linked in this order). The pterin is understood to be responsible in the receptor binding. The mechanism behind the newly increased luminescence has yet to be elucidated and is necessary in further developing these as cancer targeting fluorophores.[40]

DFT calculations were used together with experimental measures to understand how FA evolves through hydrothermal treatment.[40] (It should be noted that gel electrophoresis performed in this case appeared to indicate particles of a molecular nature rather than nanoparticles). Optical absorption and emission spectra depicted changes in absorption at 200°C at 180 minutes with a corresponding increase in emission intensity and quantum yield, while the emission peak shape remained unchanged.[40] This indicates the HT disrupts the non-radiative relaxation pathway: the PABA is understood to absorb charge from the excited state pteridine, 'quenching' it and reducing emission, disruption of this allows greater emission. Therefore, the increased emissions suggest PABA has been affected. DFT calculations were performed at the B3LYP 6-

31G(d,p) for geometry optimization, frequency calculations including Raman intensities and TD-B3LYP for excitation wavelengths and UV-VIS spectra. SMD was used in all calculations for solvent effect.[40]

DFT was performed for the absorption spectra of different possible fragments of FA – as a means to interpret the experimental spectra –; folic acid, folic acid without the Glu, and pterine and 6-formyl pterin, the latter reflective of two different pathways of GABA breakdown from the MPT.[40] By comparing newly emergent peaks in the experimental absorption spectrum to the DFT data, these peaks are identified as 6-formyl pterin, and the increased emission a result of the PABA relaxation pathway disruption.[40]

Experimental infrared spectroscopy and Raman intensity spectra before and after treatment were compared to DFT data – IR is sensitive to polarity and the ensuing bond vibrational changes, whereas Raman identifies non polar bonds, so both are employed to further understand the molecular changes occurring.[40] IR results suggest the breakdown of the Glu part of the molecule as well as the persistence of the aromatic rings and the amino acids. DFT Raman data was employed to examine experimental results and strongly indicated the disappearance of Glu and GABA alongside the preservation of the pterin ring. This allows the conclusion that the MPT remains intact and is behind the increased emissions, and this is supported by previous studies that demonstrate that the folate receptor binding abilities persist after heat treatment.[40]

DFT was here employed as a means to interpret experimental Raman spectroscopy and absorption and emission spectra, to elucidate the possible molecular evolution of an important biomolecule under hydrothermal treatment and provided valuable insight that will allow for further research and development of targeted therapies with folic acid, in addition, the advantages of DFT based screening in fluorophore development is evident.[40]

IV Porphyrins – Fascinating Complex Molecules with a Uniquely Stable Core: An In-Depth Look at Meso-Substituted Zinc Porphyrins and the Origins of their Special Characteristics[44]

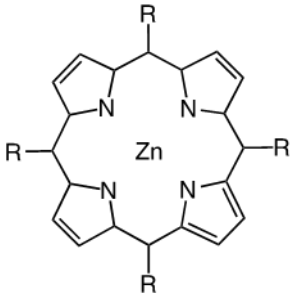

Zinc porphyrin

Porphyrins have long been a subject of fascination and crucial to life on earth. Heme is a porphyrin that binds iron and carries oxygen; chlorophyll binds magnesium in photosynthesis. These heteromacrocyclic compounds feature an aromatic conjugated system, often with a metal atom coordinated in the center and exhibit outstanding biochemical properties.[45] Their π-conjugated system, chromophore core lends them unique photophysical properties, highly excitable and absorbing strongly in the visible region, current research aims to exploit their photosensitizing abilities in areas ranging from targeted cancer therapies to solar energy conversion. Photodynamic therapy, PDT is a promising field first explored in the 1970s and relies on the therapeutic capabilities of photoexcited compounds, current research is dedicated to

developing photosensitizers – porphyrins and their synthetic analogs, phthalocyanines – that can be administered alone or together with bioactive agents in the treatment of neoplastic disease. Ideally, the porphyrins, at target sites, due to their unique properties, absorb photons, become photoexcited and in this state convert oxygen in cells into singlet oxygen (among other reactive oxygen species) which can induce cell death by reacting with various constituents in biological membranes.[45]As solar energy conversion gains increasing traction, porphyrins are being researched for their use as photosensitizing agents in solar cells, given their superior absorption in the visible spectrum, as well as the relative ease with which the structures can be modified.[46]

This study investigates a large range of zinc porphyrins that are *meso*-substituted: porphyrins consist of four pyrrole rings with their N pointing towards the center, linked by the N-adjacent C atoms of the ring with 1 C atom between each pyrrole, forming a large, π-conjugated ring.[44] These latter C atoms – *meso* carbons – are considered the weakest sites in the bonding system and substituting them has been shown to 'shield' the molecule from nucleophilic attack. Phenyl groups have been seen as an attractive candidate for this role, and as such are the focus of the research at hand, (for example, with Zn-5,10,15,20-tetrakis(3,5-di-tert-butylphenyl)porphyrin (ZnTBPP) displaying lipophilic properties that indicate its potential biological application).[44]

The structural and geometric effects of diverse phenyl groups were analyzed with crystallography and DFT, which was used to calculate the structures and infrared spectra for a sampling of Zn porphyrins. DFT has shown to be accurate and effective even which complex molecules, calculations were performed with B3LYP LANL2DZ.[44] The DFT IR was performed to provide information about the effect these substitutions would have on the dynamic behavior of the porphyrins, focusing on the bonds within the core of the macrocycle – the conjugated π system.[44] With ZnTBPP acting as the model compound – crystallographic data depicts a stable molecule with an ideal planar coordination and no distortion, this crystal data was compared to that of 105 analogs. Excellent correlation with no more than 1-2.03% discrepancy between DFT and crystal data was noted, even given the vacuum conditions of DFT. Interatomic distances for the Zn – N, C – N and bridging bonds, and the core perimeter were compared between the crystal data for ZnTBPP, DFT and the average of the surveyed analogs. Results were in excellent agreement and indicated that symmetry can be slightly distorted by different derivatives of the phenyl group, but even given this distortion, core perimeters were hardly affected, these findings indicating the inherent, superior stability of the porphyrins' core. All bonds that form a part of the conjugated system, even with distortion of the pyrrole rings, retained their stability. The equality of these bonds, too, demonstrate a uniquely well organized and flexible system, that allows for accommodation of structural distortion without adversely affecting the integral function of the molecule.[44]

DFT IR spectroscopic calculations were performed on the ZnTBPP and selected analogs, and experimental FTIR was obtained for ZnTBPP. Their comparison revealed common features and patterns with intensities deviating in some instances.[44] Given the porphyrin's system involves mutually coupled vibrations, individual modes can be difficult to identify but certain stretching areas – like the bridges – can be extrapolated and those were used in analysis, and showed general trends like 'pyrrole breathing' – pyrrole group oscillations – that can be affected by the nature of the meso substituent, the stretching vibrations of the C – C bonds involving the meso C also influenced. Where the macrocycle part of the complexes is concerned, spectral features are extremely similar with almost equal frequencies of vibrational modes for all atoms of the core and again, indicate that the π system remains impervious by the meso phenyl-substituents.[44]

DFT and experimental data provided very close results, that were qualitatively almost identical, for both the structural parameters and the IR analysis. This study conclusively detailed the inherent strength and flexibility of the tetra *meso* substituted porphyrin core and its π conjugated system that allow it to 'hold' extra energy without disrupting its stability. These attributes along with its unique chemical properties make this fascinating macrocycle a potential candidate for diverse applications.[44]

V A Comprehensive Quantum Mechanical Investigation of the yet-Inconclusive Mechanism of OH Radical Addition to Adenine – the Origins of Mutagenesis[47]

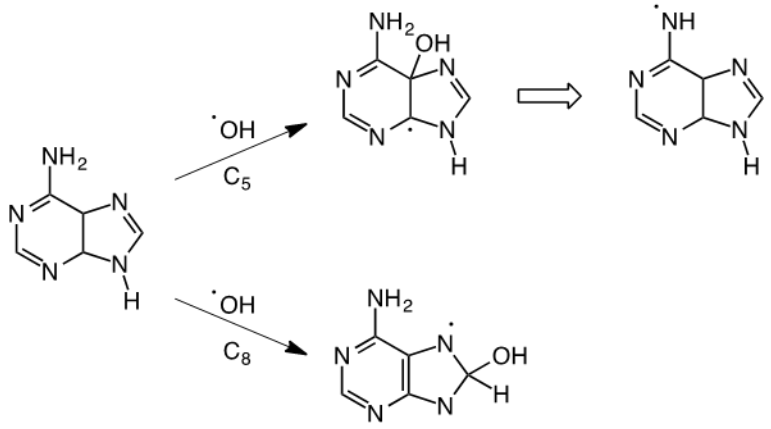

**OH addition to adenine*

ROS – reactive oxygen species – are highly unstable compounds generated in biological systems not only through regular metabolic processes, but also from solar radiation, pollution and other external sources. ROS cause cellular damage in biological systems in many ways, including the oxidizing of DNA nucleobases, the damage being central to cardiovascular disease, cancers and diabetes, as well as the effects of aging.[47] The *OH (hydroxy radical) is the species most liable in DNA injury, causing nucleobase damage, sugar backbone damage due to hydrolysis of the N – glycosyl link that weakens it, as well as radicals contained on the bases interacting with ribose sugars forming ribose radicals and eventually causing strand breakage,[48] and enabling crosslinking with proteins. The study[47] at hand looks at adenine base lesions; these can be formed at all nucleobases by the addition of hydroxyl radicals, which in turn cause different hydrogen bonding patterns compared to their parent strands and interfere with polymerase activity on the opposite strand – incorrect base pairing – and unrepaired, this a potential first step in carcinogenesis and mutagenesis.[48]

*OH reactivity with nucleobases has been widely studied but the mechanistic pathways of these reactions have not been described conclusively across the literature. In general, *OH reacts with DNA/RNA through one-electron oxidation, addition across various double bonds, and H atom abstraction. The radical addition to adenine has been proposed[48] to proceed along two main pathways: 1. addition at the C4 position to form A4OH* followed by dehydration to produce the A(-H)*; and 2. Addition at the C8 position forming the A8OH* adduct that is followed by a ring opening. It is also proposed that the A(-H)* – an oxidizing agent due to spin density about the Ns – is repaired by reducing agents deriving from the A8OH*. These findings were based primarily on absorption spectra of an adenine derivative and *OH taken at differing pH levels,

at 2-8 μs and then again at 30-260 μs which revealed a build-up of peaks at 330nm and decay at 400nm and attributed to the ring opening of A8OH* and dehydration of A4OH* respectively.[49]

Essentially unaccounted for in research is the possibility of C5 addition to A5OH* also dehydrating to A(-H)*.The hydrogenation occurs at the NH2 site, forming the radical ANH species, which, as later studies – including TD-DFT computations – find, is characterized by signals near the 330nm wavelength as well as in the ~450-550nm region,[50] which brings into question the original attribution of the peaks. Another discrepancy is also noted; O_2 quenching as well as other parameters indicate that the ~330 nm and ~400 nm signals belong to two separate processes. The subject research takes a computational approach using M06-2X with 6-31++G(d,p) for thermodynamics, frequency calculations for energy minima and TSs and IRC to connect products and reactants through TSs, followed by further optimization of IRC final structures. IEF-PCM was used for solvent effects, as well as explicit water molecules included in relevant numbers for particular reactions. For optimal accuracy, energy corrections were performed using (the coupled cluster method with single, double, and perturbative triple excitations) CCSD(T) which proved highly comparable to the less computationally expensive M06-2X-PCM and validated its use, though the CCSD(T) was used for the electron transfer reactions.[47]

VAEs – vertical absorption energies – for all radical intermediates were calculated with CASPT2//CASSCF – complete active space second-order perturbation theory (energies corrected)//complete active space self-consistent field (geometries optimized) (for more computation details refer to paper, ref [47]).

The chemistry of the *OH addition to adenine was explored for the C4 (A4OH), C5 (A5OH) and C8 (A8OH) sites and their (predicted) ensuing reaction mechanisms.[47] Addition at the first two sites is followed by a loss of OH- forming a radical cation, which loses H^+ to form the ANH radical (that can be reduced back to adenine through a one electron transfer and H^+), or the less energetically favored A2C radical. The A8OH radical addition can be followed by one-electron transfer and either reduction or oxidation for HA (7-hydro-8-hydroxypurine) and 8-oxoAoh products respectively (see paper, ref.). It can also be followed with water-assisted H-transfer (to the N7 site) forming the radical zwitterion A8ZW that can be oxidized to 8-oxoAco, or, can undergo ring opening to form the A8N9a radical (that through water-assisted H-transfer to the N9 site forms an N7 site radical A8FORMa, also) in turn reduced to FAPyA. FAPya and 8-oxoAoc/8-oxoAoh are known mutagens.[47] For each product, reactant and intermediate, ΔG and $G^{\ddagger}$ energies (kcal/mol) are computed, using M06-2X-(PCM), except the G values of $A^{\bullet+}$, ANH, and A2C, which are computed using CCSD(T)-(PCM)//M06-2X-(PCM). For each, vertical absorptions (electronic transitions) (λ, in nm) are calculated with CASPT2//CASSCF.[47] The reported energies of the radical intermediates are relative to the A (G=0) + •OH reactants. ΔG values are calculated for all one-electron transfer and deprotonation and protonation reactions, including those water-assisted.[47]

O_2 quenching is used to trap organic radicals, and experimental data was used to infer a ratio of the addition products from adenine and the OH radical; supplemented by Mulliken calculations performed for spin densities – looking at the distribution over different radicals for O_2 reactivity. Spin density overlying C atoms vs N atoms makes the species more reactive with O_2.[47]

One-electron transfer reactions, which feature in various pathways, were computed at different pH values in order to have a comprehensive understanding of these radical reactions in order to accurately apply it to the biological environment (see authors' comments on this subject).[47]

This comprehensive computational approach allowed a complete reinterpretation of experiments and research over the past decades, showing, based on thermodynamics, Gibbs free energy activation barriers and the highly accurate multiconfigurational vertical excitation energies for the radical intermediates, leading to the following conclusions:

Almost exclusively, the addition products are the A5OH and A8OH. The A8OH radicals undergo ring opening followed by oxidation or reduction forming the mutagens 8-oxoA and FAPyA, all through various steps and intermediates. A8OH and its ring-opened radical derivatives absorb at around ~400 nm and the decay noted at that wavelength is caused by their oxidation and reduction. The ANH radical is responsible for the buildup observed at ~330 nm. A4OH is determined to be a very minor radical addition product, in contradiction to previous studies. Overall, yield of *OH addition to adenine in aqueous solution has been determined to be around 44.5%. The research aspects surrounding the pH dependence, among other predictions, depict the hydrophobic environment of DNA as a facilitator of the mutagen product formation.[47]

7. CONCLUSION

This representative group of studies illustrates how computational chemistry is applied to gain an understanding of reaction progress, to explain observed trends and phenomena and to predict reactivity down to very specific aspects. Many varied studies have demonstrated highly dependable correlation between computational and experimental results, proving the value in this treatment, while in many other cases, quantum-based chemistry yields results that are otherwise unattainable or difficult to achieve experimentally. It has become an essential approach to researching the broad and fascinating chemistry of nitrogen-containing organic compounds, giving a unique insight into cycloaddition and bioorthogonal reactions, their aromaticity, photochemistry, their roles in biological processes and as building blocks of biomolecules and their other inherent complex chemistry. The computational approach is a new frontier, a fast-evolving field that provides a singular new look into the world of chemistry, demonstrated here through the lens of poly-nitrogen compounds.

8. CITATIONS

[A] Jose Sosa, Maria. “Mono- and Bis-Alkylated Lumazine Sensitizers: Synthetic, Molecular Orbital Theory, Nucleophilic Index and Photochemical Studies.” Photochemistry and Photobiology 97.1 (2021): 80–90. Web.

[B] Tanimoto, Hiroki. “Recent Applications and Developments of Organic Azides in Total Synthesis of Natural Products.” Natural product communications. 8.7 (2013): 1021–1034. Print.

[C] Dembitsky, Valery M. “Pharmacological and Predicted Activities of Natural Azo Compounds.” Natural Products and Bioperspecting 7.1 (2017): 151–169. Web.

[D] Canakci, Dilek. “Synthesis and Cytotoxic Activities of Novel Copper and Silver Complexes of 1,3-Diaryltriazene-Substituted Sulfonamides.” Journal of Enzyme Inhibition and Medicinal Chemistry 34.1 (2019): 110–116. Web.

[E] Silverman, Richard B. “Chem 316: The Organic Chemistry of Drug Design and Drug Action.” Abstracts of Papers of the American Chemical Society. Vol. 232. N.p., 2006. 197–197. Print.

[F] Naim, Mohd Javed. “Current Status of Pyrazole and Its Biological Activities.” Journal of Pharmacy and Bioallied Sciences 8.1 (2016): 2–17. Web.

[G] National Center for Biotechnology Information (2021). PubChem Compound Summary for CID 795, Imidazole. Retrieved December 2, 2021 from https://pubchem.ncbi.nlm.nih.gov/compound/Imidazole

[H] Yadav, Sanjai Kumar. “Computational Investigations and Molecular Dynamics Simulations Envisioned for Potent Antioxidant and Anticancer Drugs Using Indole-Chalcone-Triazole Hybrids.” DNA repair 86 (2020): n. pag. Web.

[I] Bonandi, Elisa. “The 1,2,3-Triazole Ring as a Bioisostere in Medicinal Chemistry.” Drug discovery today. 22.10 (2017): 1572–1581. Web.

[J] Doan, Vincent. “Electrostatic Activation of Tetrazoles.” The Journal of Organic Chemistry.85.15 (2020): 10091–10097. Web.

[K] Straughan, Donald W. “Replacement Alternative and Complementary In Vitro Methods in Pharmaceutical Research” In Vitro Methods in Pharmaceutical Research, Academic Press, (1997): Pages 1-13

[L] Prasher, Parteek. “Hybrid Molecules Based on 1,3,5-Triazine as Potential Therapeutics: A Focused Review.” Drug Development Research 81.7 (2020): 837–858. Web.

[M] Vishnu Ji Ram, “Six-Membered Heterocycles” The Chemistry of Heterocycles, Elsevier,(2019): Pages 3-391

[N] Wu, Haoxing. “Advances in Tetrazine Bioorthogonal Chemistry Driven by the Synthesis of Novel Tetrazines and Dienophiles.” ACCOUNTS OF CHEMICAL RESEARCH 51.5 (2018): 1249–1259. Web.

[1] Greer, Edyta M., Kwon, Kitae “Overview of Computational Methods for Organic Chemists.” Applied Theoretical Organic Chemistry, pp. 31-67 (2018)

[2] Boys, SF. “Electronic Wave Functions .1. A General Method of Calculation for the Stationary States of any Molecular System.” Proceedings of the Royal Society of London. 200.1063 (1950): 542–554. Web.

[3] Kohn, W. “Self-Consistent Equations Including Exchange and Correlation Effects.” Physical review online archive. 140.4A (1965): 1133–&. Web.

[4] Jabeen, Sobia. “Design, Synthesis and Application of Triazole Ligands in Suzuki Miyaura Cross Coupling Reaction of Aryl Chlorides.” Journal of molecular structure 1206 (2020): n. pag. Web.

[5] Miyaura, N. “The Palladium-Catalyzed Cross-Coupling Reaction of Phenylboronic Acid with Haloarenes in the Presence of Bases.” Synthetic Communications 11.7 (1981): 513–519. Web.

[6] Wu, Xiao-Feng “From Noble Metal to Nobel Prize: Palladium-Catalyzed Coupling Reactions as Key Methods in Organic Synthesis.” Angewandte Chemie International Edition 49.48 (2010): 9047–9050. Web.

[7] Bahsis, Lahoucine. “Clicking Azides and Alkynes with Poly(pyrazolyl)borate-Copper(I) Catalysts: An Experimental and Computational Study.” Catalysts 9.8 (2019): n. pag. Web.

[8] Kolb, HC. “Click Chemistry: Diverse Chemical Function from a Few Good Reactions.” Angewandte Chemie-International Edition 40.11 (2001): 2004–+. Web.

[9] “On the Nature of Parr Functions to Predict the Most Reactive Sites Along Organic Polar Reactions.” Chemical physics letters 582 (2013): 141–143. Web.)

[10] Hamzehloueian, Mahshid. “A Theoretical Study on the Metal-Free Triazole Formation through Tandem [3+2] Cycloaddition/retro-Diels-Alder Reaction of Benzyl Azide and Oxanorbornadienedicarboxylate.” Journal of molecular graphics and modelling. 97 (2020): n. pag. Web.

[11] Vocadlo, DJ. “A Chemical Approach for Identifying O-GlcNAc-Modified Proteins in Cells.” Proceedings of the National Academy of Sciences of the United States of America. 100.16 (2003): 9116–9121. Web

[12] Houszka, Nicole et al. “Chemoselectivity of Tertiary Azides in Strain-Promoted Alkyne-Azide Cycloadditions.” Chemistry : a European journal. 25.3 (2019): 754–758. Web.

[13] Ribeiro, Antonio M. P. et al. “Total Facial Discrimination of 1,3-Dipolar Cycloadditions in a D-Erythrose 1,3-Dioxane Template: Computational Studies of a Concerted Mechanism.” Journal of Organic Chemistry 82.2 (2017): 982–991. Web

[14] Yang, Yun-Fang. “Computational Exploration of Concerted and Zwitterionic Mechanisms of Diels-Alder Reactions Between 1,2,3-Triazines and Enamines and Acceleration by Hydrogen-Bonding Solvents.” Journal of the American Chemical Society. 139.50 (2017): 18213–18221. Web.

[15] Zhang, Jiajun. “Inverse Electron Demand Diels-Alder Reactions of Heterocyclic Azadienes, 1-Aza-1,3-Butadienes, Cyclopropenone Ketals, and Related Systems. A Retrospective.” Journal of Organic Chemistry 84.15 (2019): 9397–9445. Web.

[16] Xie, Sheng. “1,3-Dipolar Cycloaddition Reactivities of Perfluorinated Aryl Azides with Enamines and Strained Dipolarophiles.” Journal of the American Chemical Society. 137.8 (2015): 2958–2966. Web

[17] Liu, Fang. “Bioorthogonal Cycloadditions: Computational Analysis with the Distortion/Interaction Model and Predictions of Reactivities.” Accounts of Chemical Research 50.9 (2017): 2297–2308. Web.

[18] Ess, Daniel H. “Distortion/Interaction Energy Control of 1,3-Dipolar Cycloaddition Reactivity.” Journal of the American Chemical Society. 129.35 (2007): 10646–+. Web.

[19] Ess, Daniel H. “Theory of 1,3-Dipolar Cycloadditions: Distortion/interaction and Frontier Molecular Orbital Models.” Journal of the American Chemical Society. 130.31 (2008): 10187–10198. Web.

[20] Vocadlo, DJ. “A Chemical Approach for Identifying O-GlcNAc-Modified Proteins in Cells.” Proceedings of the National Academy of Sciences of the United States of America. 100.16 (2003): 9116–9121. Web.

[21] Nguyen, Sean S. et al. “Isomeric Triazines Exhibit Unique Profiles of Bioorthogonal Reactivity.” Chemical Science 10.39 (2019): 9109–9114. Web.

[22] Kamber, David N. “1,2,4-Triazines Are Versatile Bioorthogonal Reagents.” Journal of the American Chemical Society. 137.26 (2015): 8388–8391. Web.

[23] Kang, Young Kee. “Allylic Azide Rearrangements Investigated by Density Functional Theory Calculations.” Bulletin of the Korean Chemical Society 38.12 (2017): 1419–1426. Web

[24] Joshi, Sameer M. “Synthesis of Radiolabelled Aryl Azides from Diazonium Salts: Experimental and Computational Results Permit the Identification of the Preferred Mechanism.” Chemical Communications 51.43 (2015): 8954–8957. Web.

[25] Bednarek, Christin. “The Staudinger Ligation.” Chemical Reviews 120.10 (2020): 4301–4354. Web.

[26] Potential Energy Surfaces. (2016, April 3). https://chem.libretexts.org/@go/page/20275

[27] Ning, Yongquan et al. “Neighbouring Carbonyl Group-Assisted Sequential 1,2-Azide and 1,4-Oxygen Migrations of Vinyl Azides Leading to Alpha-Azido Ketones.” Science-China Chemistry 63.4 (2020): 460–466. Web.

[28] Keshavayya, J. et al. “Synthesis, Characterization, Computational and Biological Studies of Nitrothiazole Incorporated Heterocyclic Azo Dyes.” Structural Chemistry 31.4 (2020): 1317–1329. Web.

[29] Sener, Nesrin. “A Combined Experimental and DFT Investigation of Disazo Dye Having Pyrazole Skeleton.” Journal of molecular structure 1129 (2017): 222–230. Web.

[30]Oliveira, Aline A. et al. “Crystal Packing of a zinc(II)-Azide Complex with a N,N,S-Tridentate Thiosemicarbazone Ligand: An Experimental and Computational Study.” Journal of Molecular Structure 1197 (2019): 393–400. Web.

[31] Beraldo, H. “The Wide Pharmacological Versatility of Semicarbazones, Thiosemicarbazones and Their Metal Complexes.” Mini-Reviews in Medicinal Chemistry 4.1 (2004): 31–39. Web.

[32] Lee, Changsuk, Benjamin G. Janesko, and Eric E. Simanek. “Triazine-Substituted and Acyl Hydrazones: Experiment and Computation Reveal a Stability Inversion at Low pH.” Molecular Pharmaceutics 12.8 (2015): 2924–2927. Web.

[33] Kakeshpour, Tayeb. “AMHB: (Anti)aromaticity-Modulated Hydrogen Bonding.” Journal of the American Chemical Society. 138.10 (2016): 3427–3432. Web.

[34] Sola, Miquel. “Forty Years of Clar’s Aromatic Pi-Sextet Rule.” Frontiers in Chemistry 1 (2013): n. pag. Web.

[35] Kakeshpour, Tayeb. “High-Field NMR Spectroscopy Reveals Aromaticity-Modulated Hydrogen Bonding in Heterocycles.” Angewandte Chemie – International Edition 56.33 (2017): 9842–9846. Web.

[36] Wu, Chia-Hua. “Excited-State Proton Transfer Relieves Antiaromaticity in Molecules.” Proceedings of the National Academy of Sciences of the United States of America. 116.41 (2019): 20303–20308. Web.

[37] Baird, NC. “Quantum Organic Photochemistry .2. Resonance and Aromaticity in Lowest Pi-3-Pi] State of Cyclic Hydrocarbons.” Journal of the American Chemical Society. 94.14 (1972): 4941–&. Web.

[38] Szatylowicz, Halina. “Substituent Effects on the Stability of the Four Most Stable Tautomers of Adenine and Purine.” RSC Advances 9.54 (2019): 31343–31356. Web

[39] Martin, Christopher B. “Density Functional Theory Study of Possible Mechanisms of Folic Acid Photodecomposition.” Journal of photochemistry and photobiology. 208.1 (2009): 1–6. Web.

[40] Abramova, Anna M. “Molecular Nature of Breakdown of the Folic Acid Under Hydrothermal Treatment: a Combined Experimental and DFT Study.” Scientific Reports 10.1 (2020): n. pag. Web.

[41] Chen, Chen. “Structural Basis for Molecular Recognition of Folic Acid by Folate Receptors.” Nature. 500.7463 (2013): 486–+. Web.

[42] Liu, Haifang. “Synthesis of Luminescent Carbon Dots with Ultrahigh Quantum Yield and Inherent Folate Receptor-Positive Cancer Cell Targetability.” Scientific Reports 8 (2018): n. pag. Web.

[43] Chung, Seokhwan. “Graphene Quantum Dots and Their Applications in Bioimaging, Biosensing, and Therapy.” Advanced Materials 33.22 (2021): n. pag. Web.

[44] Slota, Rudolf. “Structural and Molecular Characterization of Meso-Substituted Zinc Porphyrins: A DFT Supported Study.” Molecules 16.12 (2011): 9957–9971. Web.

[45] Janas, Katarzyna. “Porphyrin and Phthalocyanine Photosensitizers Designed for Targeted Photodynamic Therapy of Colorectal Cancer.” Bioorganic & medicinal chemistry. 30 (2021): n. pag. Web.

[46] Olteanu, Liviu. “Palladium(II)-Porphyrin Complexes as Efficient Sensitizers for Solar Energy Conversion.” Journal of Science and Arts 2 (2021): 557–568. Print.

[47] Frances-Monerris, Antonio. “Mechanism of the OH Radical Addition to Adenine from Quantum Chemistry Determinations of Reaction Paths and Spectroscopic Tracking of the Intermediates.” Journal of Organic Chemistry 82.1 (2017): 276–288. Web.

[48]Breen, AP. “Reactions of Oxyl Radicals with DNA.” Free radical biology & medicine. 18.6 (1995): 1033–1077. Web.

[49]Vieira, AJSC. “Pattern of OH Radical Reaction with Adenine and its Nucleosides and Nucleotides – Characterization of 2 Types of Isomeric OH Adduct and their Unimolecular Transformation Reactions.” Journal of the American Chemical Society. 112.19 (1990): 6986–6994. Web.

[50] Banyasz, Akos. “UV-Induced Adenine Radicals Induced in DNA A-Tracts: Spectral and Dynamical Characterization.” Journal of Physical Chemistry Letters 7.19 (2016): 3949–3953. Web.

[51] Jose Sosa, Maria. “Mono- and Bis-Alkylated Lumazine Sensitizers: Synthetic, Molecular Orbital Theory, Nucleophilic Index and Photochemical Studies.” Photochemistry and Photobiology 97.1 (2021): 80–90. Web.